DETERMINATION OF VISCOSITY OF OIL BY FALLING-SPHERE METHOD USING DIGITAL-IMAGING SYSTEM

By

Getachew Asmelash

SUBMITTED IN PARTIAL FULFILLMENT OF THE
REQUIREMENTS FOR THE DEGREE OF
MASTER OF SCIENCE IN PHYSICS
AT
ADDIS ABABA UNIVERSITY
ADDIS ABABA, ETHIOPIA
JUNE 2009

ADDIS ABABA UNIVERSITY
DEPARTMENT OF
PHYSICS

The undersigned hereby certify that they have read and recommend to the School of Graduate Studies for acceptance a thesis entitled "**Determination Of viscosity of oil by falling-sphere method using digital-imaging system**" by **Getachew Asmelash** in partial fulfillment of the requirements for the degree of **Master of Science in Physics**.

Dated: June 2009

Supervisor: _____
Dr. Araya Asfaw

Examiners: _____
Dr. Mulugeta Bekele

_____
Prof. A.V.Golap

ADDIS ABABA UNIVERSITY

Date: **June 2009**

Author: **Getachew Asmelash**

Title: **Determination Of viscosity of oil by falling-sphere method using digital-imaging system**

Department: **Physics**

Degree: **M.Sc.** Convocation: **June** Year: **2009**

Permission is herewith granted to Addis Ababa University to circulate and to have copied for non-commercial purposes, at its discretion, the above title upon the request of individuals or institutions.

Signature of Author

This work is gratefully dedicated to " Weladite Amlak, without whose support, not a word would have been written!.

Table of Contents

List of Figures

Abstract

Viscosity is the most important physical property for lubricating oils. The measurement of viscosity resists on the velocity limit measurement of falling-ball, corrected principal identified effects (edge or wall effects, inertial effects, and end effects).

In this research falling-sphere technique is used to measure the viscosity of Total quartz 20W50 motor oil by monitoring the terminal velocity at which a sphere falls under gravity in a cylindrical tube containing the test fluid. The experiments, the sphere is monitored using video system and the position coordinate and time are measured.

The principal difficulties with this system are the measurement of the velocity of the ball. The result of the experiment agree with the theoretical values and reported value by Total oil company, even-though, there are uncertainties in measurement of falling velocity, corrected terminal velocity, density of sphere, and fluid and radius.

Acknowledgements

Above all, I would like to thank the almighty; God, for letting me accomplish this stage.

I would like to express my gratitude to Dr. Araya Asfaw, my advisor, for his suggestions; constant guidance; constructive criticism; lending his own valuable books to use as reference and editing the manuscript and friendly approach during this research. His tireless follow up and his consistent support will be in my memory forever.

My gratefulness thanks and appreciation also extended to Tesfaye Mamo, technical assistance. I also appreciate his friend, Hiwot, for lending her own CCD camera and Dessalegn Taddesse, Kassahun Ture, Dilu, and Hibret for their valuable suggestions and help in this research work.

My strongest thank is addressed to my family, who lived for my self. They are the hero of my success with out their support and hope, this stage is unthinkable. I wish also thankful to Aron, and Temesgen, for their best friendship. I have derived materials from many research journals and books, and am indebted to the authors of those publications and books.

Last but not least, I am also thankful to Abebe Adugna and Firehiwot Aregawi for his and her patient support in collecting and sending my salary for entire two years.

Introduction

The measurement of the fluid viscosity is now day important in many industrial processes such as forming of polymer composites, manufacturing of varnishes, cosmetics, certain food products and various suspensions. One of the devices for measuring viscosity is a falling sphere viscometry. There are various measurement techniques like the capillary or rotary rheometry. The viscosity laboratory of BNM-LNM provides reference oils, calibrate capillary tube viscometries of all types to ensure the traceability of national standards. Materialization of the national range of viscosity is based on the kinematics viscosity of bi-distilled water at 20^0c ($1.0034\frac{mm^2}{sec}$). This value can be used to calibrate primary U- tube viscometries, which are used to calibrate the ubbelhode type work viscometries.

The main disadvantage of capillary viscometry, used in many laboratories, including the BNM-LNE[1], is the increase in uncertainty at each step of the step-up procedure [1], particularly with high viscosities routinely found in industry. Moreover, the procedure is based on knowledge of the viscosity of water.

Viscosity is one of the most important physical properties for lubricating oils. Lubricant oil is used to separate two surfaces that are moving with respect to each other. Viscosity is a principal parameter when any flow measurements of fluids, such as liquids, semi-solids, gases and even solids are made. Viscosity measurement are

made in conjunction with product quality and efficiency. Manufacturers now regard viscometers as a crucial parts of their research development and process control programs. They know that viscosity measurements are often the quickest, most accurate and most reliable way to analyze some of the most important factors affecting product performance. Practically viscosity is measured based on different physical principles. These are capillary viscometer, rotational viscometer, falling(or rising) sphere viscometer, cone-and-plate viscometer, concentric cylinder viscometer.

In this present research work all correction factor which are wall effects, end effects, and edge effects are included into consideration in order to determine the viscosity of incompressible viscous fluid by measuring the terminal velocity of the spheres which is monitored using video system. The result of the experiment agrees with the theoretical values and reported value by Total oil company.

Moreover, viscosity and terminal velocity of a falling ball can be determine by falling-sphere viscometer using laser system which have done by ,Getachew Work, last year. In his work, first he proposed a stream function and from it, axial and radial component of velocities are calculated through restriction imposed on boundary values and continuity equation. The velocity components are inserted into momentum equation, finally he develop new expression of viscosity to calculate dynamic viscosity of fluids. However, the main encountered with this method is the measurement of the terminal velocity of the ball and corrections to componsate for the effects exercised on the ball.

Knowledge of the terminal velocity of solid sphere falling in liquid is required in many industrial applications, like oil well drilling, hydraulic transport slurry systems for coal and ore transportation, thickeners, mineral processing, and geothermal

drilling.

The objective of this research is two-fold: first to improve on the method for determining the terminal velocity of the falling ball by a falling-sphere viscometer using laser system built in our laboratory by Getachew Worku[2008], and the second to determine the viscosity of Total quartz 20W50 motor oil an incompressible fluid by using the data obtained in the experiment.

The thesis has five chapters. Chapter 1 presents theory on the fluid mechanics and theory formulation on a single fluid model. In chapter 2, different types of viscometers used to determine viscosity are reviewed.

Chapter 3 the experimental system for falling sphere viscometer using digital imaging system to measure the terminal velocity is described. The results of the experiment will be presented in chapter 4. In chapter 5 concluding remarks and recommendation are given.

The rules used to estimate the experiments errors are given in appendix A. A Matlab computer code used to plot the velocity profile is provided in appendix B. Appendix C is a program using Matlab to estimate the uncertainty in the measurement of the terminal velocity and viscosity.

Chapter 1

Fluid mechanics and Fluid dynamics

Fluid mechanics is a discipline within the broad field of applied mechanics concerned with the behavior of liquid and gases at rest or in motion. The analysis of the behavior of fluid is based on the fundamental law of mechanics which relate continuity of mass and energy with forces and momentum together with the familiar solid mechanics. While fluid dynamics concerns with the study of the motion of fluids(liquid and gases). Since the phenomena considered in fluid dynamics are macroscopic, a fluid is regarded as a continuous medium.

1.1 Fluid

Fluid is defined as a substance that deforms continuously when acted on by a shear stress of any magnitude. A shear stress (forces per unit area) is created whenever a tangential force acts on a surface. A plastic solid is deformed continuously during the application of a force. Once the body is free from the force, the fluid stops deformation(nominally at rest). By contrast, the fluid keeps deforming even when

it is free from force. A body of fluid is composed of innumerably many microscopic molecules. However in macroscopic world, it is regarded as a body in which mass is continuously distributed. Motion of a fluid, i.e. flow of a fluid, is considered to be a mass flow involving its continuous deformation. Fluid mechanics studies such flow of fluid, i.e. motion of material bodies of continuous mass distribution, under fundamental law of mechanics.

There are two aspects of fluid mechanics which makes it different from solid mechanics;

1. The nature of fluid is much different from that of a solid

2. In fluid we usually deal with continuous streams of fluid without a beginning

Normally,We recognize three states of matter: solid, liquid, and gas. However, liquid and gas are both fluids in contrast to solids since they lack the ability to resist deformation. Because a fluid cannot resist the deformation force, it moves; it flows under the action of a force. Its shape will change continuously as long as a force is applied. A solid can resist a deformation force while at rest, this force may cause some displacement but the solid does not continue to move indefinitely. The fundamental property of a fluid is that it cannot be in equilibrium state of a stress such that the mutual action between two adjacent parts is oblique to the common surface. This property is the basis of hydrostatics. Let us suppose for instance that a vessel in the form of a circular cylinder, containing water (or other liquid), is made to rotate about its axis, which is vertical.

If the angular velocity of the vessel is constant, the fluid is soon found to be rotating with the vessel as one solid body. If the vessel is brought to rest, the motion of the fluid continuous for some time, but gradually subsides, at length and ceases

altogether. These phenomena point to the existence of mutual action between contiguous elements which are partly tangential to the common surface. If the mutual action were every where wholly normal, it is obvious that the moments of momentum, about the axis of vessel, of any portion of fluid bounded by a surfaces of revolution about this axis, would be constant. We infer, moreover, that those tangential stresses are not called into play so long as the fluid moves as a solid body, but only whilst a change of shape of some portion of the mass is going on, and that their tendency is to oppose this change of shape.

1.1.1 Stress, Pressure

The macroscopic concepts of internal forces and stress which are used in solid-body mechanics are carried over to fluid mechanics. The forces that act on a fluid element can be classified as either body forces or as surface forces. Body forces are forces that are distributed throughout the material and act at a distance. Gravitational and electromagnetic forces are classified as body forces. Surface forces are contact forces that act, as the name implies, on a surface. To develop the concept of stress, we will examine the internal force that one part of the fluid exerts on the other across an infinitesimal surface.

In a gas, it is postulated (in the kinetic theory of gases) that internal forces result from molecular transport across this surface. This result in a transfer of momentum. The net rates of momentum transfer is equivalent to a force. Since the internal force may vary from point to point, we subdivided the cutting surface into infinitesimal elements and consider the force, $\triangle F$ that acts on area $\triangle A$. Now the magnitude of $\triangle F$ depends on the size of $\triangle A$, and thus it cannot be considered a field quantity.

The surface traction, or stress vector, designated as τ, is a field quantity and is thus a more convenient term to use in continuum mechanics.The quantity $\tau(p)$ does not depend on the size of $\triangle A$ and is defined as a limit, as $\triangle A$ goes to zero around point P; that is,

$$\vec{\tau(p)} = \lim_{\triangle A \to (0)} \frac{\triangle F}{\triangle A} \tag{1.1.1}$$

If point P is held constant but the orientation of $\triangle A$ changes, so does the surface traction is also change.

The surface traction, τ is often decomposed into two components, normal and tangent to the surface, designated as, τ_n and τ_t respectively as shown in (Fig1.1). Thus $\tau(p)$ can be written as;

$$\vec{\tau(p)} = \tau_n(p)\hat{e_n} + \tau_t(p)\hat{e_t} \tag{1.1.2}$$

where $\hat{e_n}$ and $\hat{e_t}$ are, respectively, the unit vector normal and tangent to the surface $\triangle A$.

The component τ_n is called the normal stress, and the component τ_t is called

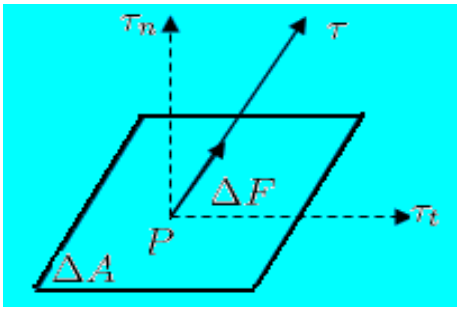

Figure 1.1: Surface traction, normal stress, and shear stress

shear stress. Normal stress is classified as either tensile (pointing out ward from the retained region) or compressive (pointing inwards toward the retained region), Since

a fluid cannot sustain any significant tensile stress, τ_n will normally be negative. In a static fluid the force per unit area that acts normal to a surface is called pressure, since the characteristics of pressure and normal stress are the same, we may take

$$\tau_n = -p \tag{1.1.3}$$

1.2 Viscosity

Viscosity is the measure of the internal friction of a fluid. This friction becomes apparent when a layer of fluid is made to move in relation to another layer. The greater the friction, the greater the amount of force required to cause this movement, which is called shear. Shear occurs whenever the fluid is physically moved or distributed, as in pouring, spreading, spraying, mixing, etc. Highly viscous fluids, therefore, require more force to move than less viscous materials.

Viscosity is a basic fluid property which is often required by engineers to make estimate of transport behavior such as mass and heat transfer. It appears in many of the engineering correction (example Reynolds number), it causes internal fluid friction. It also makes fluid stick to solid surfaces. Shear forces are transmitted through a fluid by it viscosity. Molecules of fluid exerts forces of attraction on each others. In liquid it is strong enough to keep the mass together but not strong enough to keep it rigid. In gases these forces are very weak and cannot hold the motion together.

The physical meaning of viscosity can be easily understood by considering a hypothetical experiment in which a material is placed between two very wide parallel plates as depicted in (Fig1.2). The bottom plate is rigid, but the upper plate is free to move. When the force $\vec{F}$ is applied to the upper plate, it will move continuously

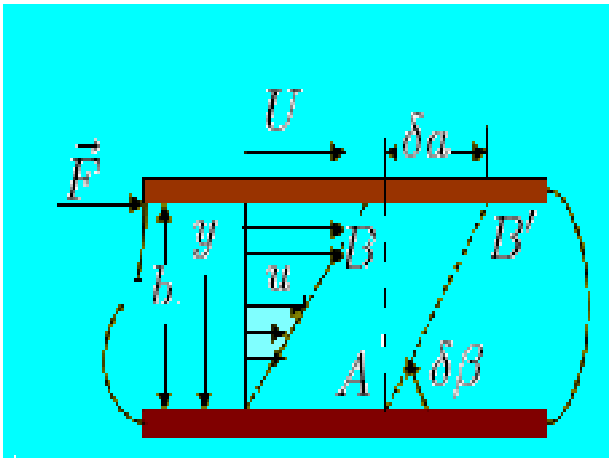

Figure 1.2: Behavior of a fluid placed between two parallel plates

with a velocity U (after the initial transient motion has died out) as illustrated in (Fig1.1). This behavior is consistent with the definition of a fluid that is, if a shear stress is applied to a fluid that it will deform continuously. A closer inspection of the fluid motion between the two plates would reveal that the fluid in contact with the upper plate moves with the plate velocity U, and the fluid in contacts with the bottom fixed plate has a zero velocity. The fluid between the two plates move with velocity $u = u(y)$ that would vary linearly, $u = \frac{U}{b}y$. Thus the velocity gradient, $\frac{du}{dy}$, develops in the fluid between the plate. In this particular case the velocity gradient is a constant, as

$$\frac{du}{dy} = \frac{U}{b}$$

but in more complex flow situation this would not be true.

The experimental observation that the fluid sticks to the solid boundaries is very important in fluid mechanics and it is usually referred to as the no-slip condition. All

fluids, both liquids and gases, satisfy this condition. In small time increment δt , an imaginary vertical line, AB in the fluid would rotate through an angle $\delta\beta$, so that

$$\tan\delta\beta \approx \delta\beta = \frac{\delta a}{b} \tag{1.2.1}$$

since

$$\delta a \;\; = \;\; U\delta t$$

It follows that

$$\delta\beta = \frac{U\delta t}{b} \tag{1.2.2}$$

In this case, $\delta\beta$ is a function not only of the force F (which governs U) but also of time. We consider the rate at which $\delta\beta$ is changing, and define the rate of shear strain, $\frac{d\gamma}{dt}$, as

$$\frac{d\gamma}{dt} = \lim_{\delta t\to 0}\frac{\delta\beta}{\delta t} \tag{1.2.3}$$

which in this instance is equal to

$$\frac{d\gamma}{dt} \;\; = \;\; \frac{du}{dy}$$

As shear stress, τ, is increased by increasing F (recall that $\tau = \frac{P}{A}$), the rate of shearing strain is increased in direct proportion-that is

$$\tau \propto \frac{du}{dt} \tag{1.2.4}$$

or

$$\tau = \eta\frac{du}{dy} \tag{1.2.5}$$

where the constant of proportionality is called the absolute viscosity, dynamic viscosity or simply the viscosity of the fluid.

Fluid for which the shear stress is linearly related to the rate of shear strain (also referred to as rate of angular deformation) are designated as Newtonian fluid while fluid for which the shear stress is not linearly related to the rate of strain are designated as non-Newtonian fluids. It is interesting to note that as in temperature increases the viscosity of a gas also increases, but in liquid the reverse occurs. In

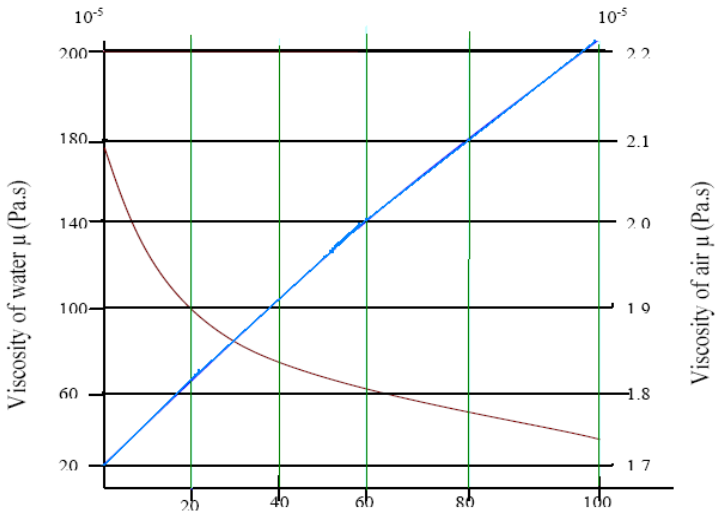

Figure 1.3: Typical viscosity versus Temperature dependence for both a gas and a liquid under 1 atm.

(Fig1.3), the viscosity of both water and air is plotted as a function of temperature.

In the kinetic theory of gases, it is theorized that the shear stress in a gas is mainly a result of molecular momentum transfer, from one layer of fluid to another. The force of attraction between molecules in a gas is small when compared with the force involved in the momentum transfer between layers. As the temperature of the

gas is increased, the molecules are further agitated, and the rate of momentum transfer is increased. In liquid, on the other hand, the cohesive force between molecules is large when compared with the momentum transfer between adjacent fluid layers. This liquid cohesive force has been found to decrease as the temperature of the liquid is raised and, hence, the shear stress and the absolute viscosity of the liquid tend to decrease under these conditions. It turns out that η and ρ appear together so often that a single term combining both quantities has been defined. This term is designated as kinematic viscosity and is defined by;

$$\nu = \frac{\eta}{\rho} \tag{1.2.6}$$

The dimension of η is $\frac{m^2}{sec}$. Fluid which does not obey eq(1.2.4) is non- Newtonian fluid which can be represented by;

$$\tau_t = k(\frac{du}{dy})^n \tag{1.2.7}$$

where k and n are constants: $n > 1$ for dilation fluids, $n < 1$ for pseudo plastic fluids, and $n = 1$, for Newtonian fluids. Plot of some for several types of non-Newtonian fluids are shown in below Fig1.4

1.2.1 Causes of viscosity in a fluid

Viscosity in liquid

There is some molecular interchange between adjacent layer in liquid, but as the molecules are so much closer than in gases the cohesive force holds the molecules in phase much more rigidly. This cohesion plays an important role in the viscosity of the liquids. Increasing the temperature of fluid reduces the cohesive forces and

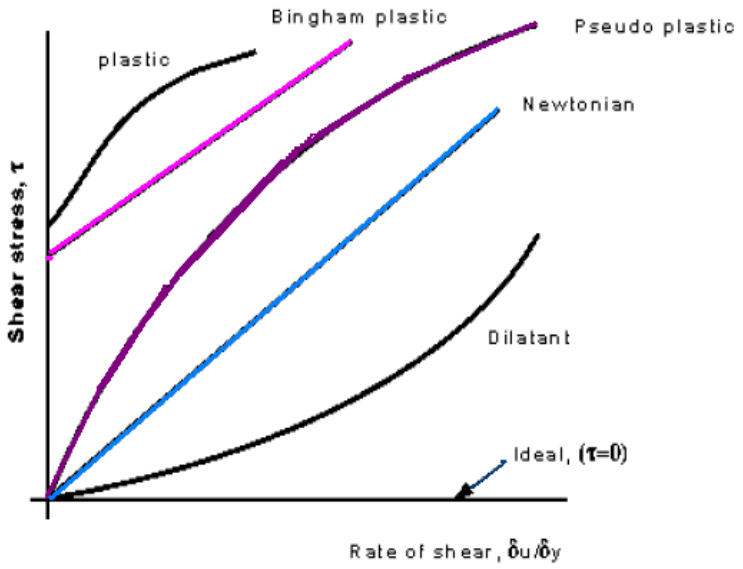

Figure 1.4: Flow curves illustrating Newtonian and non-Newtonian fluid behavior(shear stress versus strain rate)

increases the molecular interchange. Reducing cohesive force reduces shear stress, but the molecular interchange is increased. Because of this complex interrelation the effects of temperature on viscosity has something of the forms:

$$\eta_(T) = \eta_0(1 + AT + BT) \tag{1.2.8}$$

where $\eta_(T)$ is the viscosity at temperature and η_0 is the viscosity at temperature zero degree Celsius. A and B are constant for a particular fluid. High pressure can also change the viscosity of a liquid as pressure increases the relative movements of molecules which requires more energy, hence viscosity increases.

Viscosity in gases

The molecules of gases are weak in position by molecular cohesion (as they are so far apart). Since adjacent layers move on each other there is continuous exchange of molecules. Molecules of slower layers move to faster layers causing a drag, while molecules moving the other way exert an acceleration force. Mathematical consideration of this momentum exchange can lead to Newtonian law of viscosity. If the temperature of a gas increases the momentum exchange between layers will increase thus increasing viscosity.

1.3 Pressure- field equation in a static fluid

From continuum mechanics view point: take same arbitrary system occupying volume, V, in static continuum. Consider all forces acting on this system as shown in Fig1.5 Since the system is in a static equilibrium, the sum of the force acting on

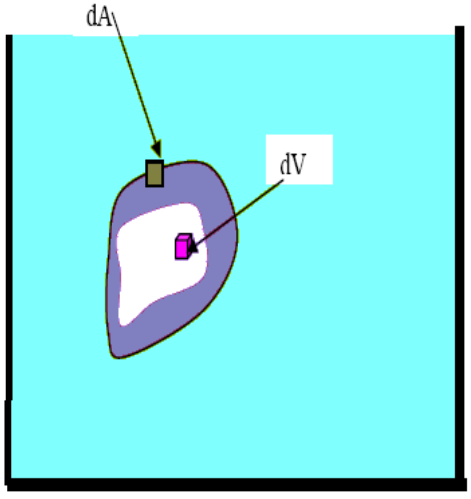

Figure 1.5: Arbitrary System in the static continuum

the system must be zero, that is,

$$-\oint_v \gamma \hat{k} dV + \oint_s \tau(s) ds = 0 \tag{1.3.1}$$

we showed that in a static fluid $\tau = -p\hat{n}$, thus;

$$\oint_s \tau(s) ds = -\oint_s p\hat{n} ds \tag{1.3.2}$$

by Green's divergence theorem:

$$\oint_s p\hat{n} ds = \oint_V \vec{\nabla} p dV \tag{1.3.3}$$

substituting eq(1.3.7), and eq(1.3.8) in to eq(1.3.6) and combining the two integrals we obtain

$$\oint_V (\gamma \hat{K} + \vec{\nabla} p) dV = 0 \tag{1.3.4}$$

Now this relationship was done for any arbitrary region in the continuum. That is

$$\gamma \hat{K} + \vec{\nabla} p \;\; = \;\; 0$$

Thus, for the integral to be zero,

$$\frac{\partial p}{\partial x} = 0, \frac{\partial p}{\partial y} = 0, and \frac{\partial p}{\partial z} + \gamma = 0 \tag{1.3.5}$$

$$\frac{\partial p}{\partial z} = -\gamma \tag{1.3.6}$$

which implies

$$p = p_0 - \gamma z \tag{1.3.7}$$

This is the governing pressure field equation in a static fluid.

1.4 Archimedes principle and buoyancy

When a body is immersed in a liquid, it losses some of its weight. When the body submerged in a liquid, the liquid exerts upward force which is known as buoyancy. The cause of buoyant force is the result of upward surface force. The surface force resulted from the pressure that the surrounding liquid exerts on the surface of the portion of the body which is submerged.

The magnitude of buoyant force on the submerged body is given by Archimedes principle which can be expressed as ;

1. a body immersed in fluid is buoyed up by a force equal to weight of fluid displaced by the body

2. a floating body displaces weight of fluid equal to its own weight [1]

To prove the first part of this principle, consider a body that is totally immersed in a liquid of density as shown below Fig1.6 The total surface force acting on the body;

$$\vec{F_s} = \oint_s \tau(\vec{s})ds = -\oint_s p\hat{n}ds \tag{1.4.1}$$

where p is the pressure field given by eq(1.3.11) when the z axis is points vertically upward ($p = z\gamma$). Then eq(1.3.33) becomes

$$\vec{F_s} = -\oint_s z\hat{n}\gamma ds \tag{1.4.2}$$

by applying Green's divergence theorem;

$$\oint_s Z\hat{n}ds \;\; = \;\; \oint_V \vec{\nabla} z dV$$

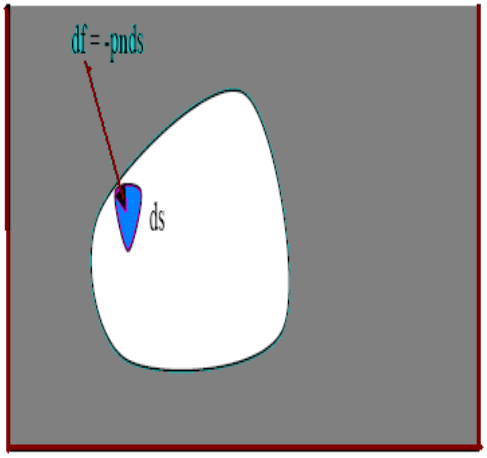

Figure 1.6: Surface force on totally submerged body

The total surface force becomes;

$$\vec{F_s} = -\gamma \oint_V \hat{k} dV = -\gamma V \hat{k} \tag{1.4.3}$$

since

$$\vec{\nabla} z \;\; = \;\; \hat{k}$$

where V is volume of the submerged body. The buoyancy force, $\vec{F_B}$, is defined as the vertical component of the resultant surface force, $\vec{F_s}$. Thus;

$$\vec{F_B} = (-\hat{k}).\vec{F_s} = -\gamma V \tag{1.4.4}$$

Notice that this formula holds true for a fluid of uniform density surrounding the body. Since the floating body is in equilibrium, the upward buoyancy force is balanced by gravitational force, thus the body displace its own weight.

1.5 Flow- field Terminology

A flow field is a region where the fluid properties (density, ρ; fluid velocity, v; pressure, p; temperature, T;etc...) may be function of the position and time. There are two view points for describing a flow field, Lagrangian and Eulerian.

1.5.1 Eulerian and Lagrangian view points

In the Lagrangian view point, a single fluid particle or element is observed as it moves through the fluid flow. This approach is invariably used in the study of particle dynamics. While in Eulerian view points, fluid particles are observed as they move into a particular point in space.

1.6 Continuity equation

It is an equation of the basic principle of the conservation of mass in a particularly convenient form for the analysis of materials processing operations. Consider a stationary volume element of length $\triangle x$, width $\triangle y$ and height $\triangle z$ in a cartesian coordinate system, as illustrated in below Fig1.7. The conservation of mass for this volume element ($\triangle V = \triangle x \triangle y \triangle z$) may be expressed verbally as;
Rate of change of mass in $\triangle V$=Rate of mass convected in to $\triangle V$ -Rate of mass convected out of $\triangle V$ expressed mathematically this is;

$$\begin{aligned} \triangle x \triangle y \triangle z) \frac{\partial \rho}{\partial t} &= \triangle y \triangle z[(\rho v_x)|_x - (\rho v_x)|_{x+\triangle x}] + \\ &\quad \triangle x \triangle z[(\rho v_y)|_y - (\rho v_y)|_{y+\triangle y}] + \\ &\quad \triangle x \triangle y[(\rho v_z)|_z - (\rho v_z)|_{z+\triangle z}] \end{aligned} \tag{1.6.1}$$

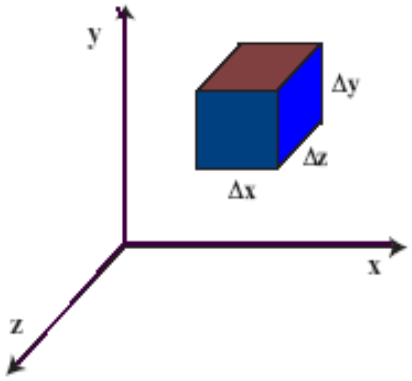

Figure 1.7: An arbitrary differential volume element

where ρ is the fluid density in $\triangle V$. Dividing each side of the eq(1.5.1) by $\triangle V$, taking limit $\triangle V \rightarrow 0$, and invoking the definition of partial derivative leads to:

$$\frac{\partial \rho}{\partial t} = -[\frac{\partial(\rho v_x)}{\partial x} + \frac{\partial(\rho v_y)}{\partial y} + \frac{\partial(\rho v_z)}{\partial z}] \tag{1.6.2}$$

This can be expressed more succinctly as;

$$\frac{\partial \rho}{\partial t} = -\vec{\nabla}.(\rho\vec{v}) \tag{1.6.3}$$

is partial derivative form of continuity equation. But the substantial derivative $\frac{D}{Dt}$ is defined as;

$$\frac{D}{Dt} = \frac{\partial}{\partial t} + \vec{v}.\vec{\nabla} \tag{1.6.4}$$

Many fluids encountered in polymer processing operations are essentially incompressible; the fluid density is constant. thus ρ is function of neither time nor space and the continuity equation reduces to;

$$\vec{\nabla}.\vec{v} = 0 \tag{1.6.5}$$

1.7 Fluid flow kinematics

kinematics implies the study of motion. Such motion is subject to the conservation of mass.

1.7.1 Stream-function

A line in the fluid whose tangent is every where parallel to $\vec{v}$ at every instant is a stream- line. Since the velocity must be tangent or parallel to the line element, and since the cross product of parallel vector is zero, the equation for the stream- line is

$$d\vec{l} \times \vec{v} = 0 \tag{1.7.1}$$

When the flow is steady, the stream lines have the same shape in all times. The flow of an incompressible fluid, or a steady flow of a compressible fluid, the continuity equation reduced to the statement that the divergence of a vector is zero. If the field is restricted to be either two dimensional(rectangular cartesian) or axially symmetrical, the divergence is the sum of only two derivatives. For the two-dimensional planer case, with $\vec{v} = (v_1, v_2, 0)$ and v_1, v_1 do not depend on z, the continuity equation has the form

$$\frac{\partial v_1}{\partial x} + \frac{\partial v_2}{\partial y} = 0 \tag{1.7.2}$$

Thus $v_1 dy - v_2 dx$ is the exact differential, call it $\Delta\psi$, and

$$v_1 = \frac{\partial \psi}{\partial y} \tag{1.7.3}$$

$$v_2 = -\frac{\partial \psi}{\partial x} \tag{1.7.4}$$

For an axial symmetric flow, the continuity equation becomes

$$\nabla.\vec{v} = \frac{\partial v_z}{\partial z} + \frac{1}{r}\frac{\partial (r v_r)}{\partial r} = 0 \tag{1.7.5}$$

In this case

$$v_1 = \frac{1}{r}\frac{\partial \psi}{\partial r} \tag{1.7.6}$$

$$v_2 = -\frac{1}{r}\frac{\partial \psi}{\partial r} \tag{1.7.7}$$

The function in this geometry is called the stokesian stream function.

1.7.2 Hydrodynamic Forces

Drag Force and Drag Coefficient:

A particle suspended in a fluid is subjected to hydrodynamic forces. For low Reynolds number, the stokes drag force on a spherical particle is given by

$$F_D = 3\pi\eta U d, \tag{1.7.8}$$

where d the particle diameter, η is the coefficient of viscosity and U is the relative velocity of the fluid with respect to the particle, eq(1.7.8) may be restated as

$$C_D = [\frac{F_D}{\frac{1}{2}\rho U^2 A}] = \frac{24}{R_e} \tag{1.7.9}$$

where ρ is the fluid density, $A = \frac{\pi d^2}{4}$ is cross sectional area of the spherical particle, and

$$R_e = \frac{\rho U d}{\eta} \tag{1.7.10}$$

is the Reynolds number.

The Stokes drag is applicable to the creeping flow regime (Stokes regime) with small Reynolds numbers ($R_e < 0.5$). At higher Reynolds numbers, the flow the drag

coefficient deviates from eq(1.7.9). Oseen[9] included the inertial effect approximately and developed a correction to the Stokes drag given as

$$C_D = \frac{24[1 + \frac{3R_e}{16}]}{R_e}, \tag{1.7.11}$$

Chapter 2

Theory formulation of a falling-sphere method

2.1 Viscosity measurement

Viscosity is the measurement of the internal friction of a fluid. This friction becomes apparent when a layer of fluid is made to move in relation to another layer. The greater the friction, the greater the amount of force required to cause this movement, which is called shear. Shear occurs, whenever the fluid is physically moved or distributed, as in pouring, spreading, spraying, mixing, etc. Highly viscous fluids, therefore, require more force to move than less viscous materials. The microscopic nature of internal friction in a fluid is analogous to the macroscopic concept of mechanical friction in the system of an objects moving in a stationary planar surface.

The resistance of a fluid to the creation and motion of flow is due to the viscosity of the fluid, which only manifests itself when motion in the fluid is set up. Consider a liquid between two closely spaced parallel plates as shown in (Fig2.1). A force, F, applied to the top plates causes the fluid adjacent to the upper plate to be dragged in the direction of F. The applied force is communicated to neighboring layers of

fluid below, each coupled to the driving layer above, but with diminishing magnitude. In this system, the applied force is called a shear (when applied over an area it is called a shear stress), and the resulting deformation rate of the fluid, as illustrated by the velocity gradient $\frac{dU_x}{dz}$, is called the shear strain rate, $\dot{\gamma}_{xx}$. The mathematical expression describing the viscous response of the system to the shear stress simply is;

$$\tau_{zx} = \eta \frac{dU_x}{dz} = \eta \dot{\gamma}_{zx} \tag{2.1.1}$$

where τ_{zx}, the shear stress, is the force per unit area exerted on the upper plate in the x-direction (and hence is equal to the force per unit area exerted by the fluid on the upper plate in the x-direction under the assumption of a no-slip boundary layer at the fluid-upper plate interface) and $\frac{dU_x}{dz}$, is the gradient of the x- velocity in the z-direction in the fluid, and η is the coefficient of viscosity. In this case, because one is concerned with a shear force that produces the fluid motion, η is more specifically called the shear dynamic viscosity.

If the viscosity throughout the fluid is independent of strain rate, the fluid is said

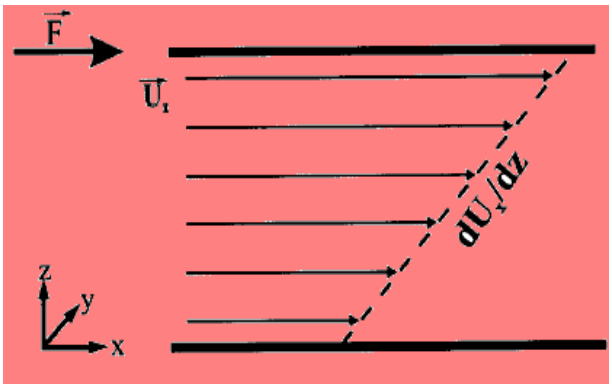

Figure 2.1: System for defining Newtonian Viscosity

to be a Newtonian fluid. Fluid deformation that is not recoverable after removal of

the stress is typical the response of viscous fluid. The other extreme response to an external stress is purely elastic and is characterized by an equilibrium deformation that is fully recovered on removal of the stress. Fluid that behave elastically in some stress range require a limiting or yield stress before they will flow as a viscous fluid. A simple, empirical, constitutive equation often used for this type of rheological behavior of the form;

$$\tau_{yx} = \tau_y + \dot{\gamma}^n \eta_p \tag{2.1.2}$$

where τ_y is the yield stress, η_p is an apparent viscosity (plastic viscosity), and exponent $'n'$ allows for a range of non-Newtonian response: $n = 1$, is pseudo-Newtonian behavior and is called Bingham fluid; $n < 1$ is shear thinning behavior; and $n > 1$ is shear thickening behavior.

2.1.1 Viscometer Types

The fluid flow in a given instrument geometry defines the strain rates, and the corresponding stresses are the measure of resistance to flow. If strain rate or stress is set and controlled, then the other one will, everything else being the same, depend on the fluid viscosity. The basic principle of all viscometry is to provide as simple flow kinematics as possible, preferably 1-D (isometric) flow, and independent of fluid type. The resistance to such flow is measured, and there by the shearing stress is determined. The shear viscosity is then easily found as the ratio between the shearing stress and the corresponding shear strain rate.

The common type of viscometers that are used to determine the viscosities at high pressures can be grouped according to the chronological development of the technique as follows;

- Capillary flow viscometer
- Rolling or Falling body viscometer
- Vibrating- Wire viscometer
- and other techniques (rotating viscometer, high pressure shear strain viscometer,)

These techniques have been widely used for measurements at high pressure and or high temperature for more than a century. In this section, the general working principle of these viscometers will be reviewed with few examples.

Capillary Flow Viscometer

Röntgen is reported to be the first to measure pressure dependence of viscosity of water. He worked with pressure up to 20bar using a capillary flow viscometer[7]. In this method a liquid is forced through a fine- bore tube, and viscosity (η) of the liquid is determined from the measured volumeteric rate($\frac{V}{t}$), the pressure drop ($\triangle p$), and the tube dimensions according to the poiseuille equation

$$\eta = \frac{\pi r^4 (\triangle p) t}{8 V l} \tag{2.1.3}$$

where r and l are the radius and the length of the capillary. This relationship is only applicable for Newtonian fluids. For non- Newtonian fluids such as those obeying Bingham- body model, power low and Eyring model, different relationships are used[8].

Barnett and Basco, in 1969, used a capillary-type viscometer which is capable of measuring up to 6GPa [1]. The design of this viscometer is under slightly different

pressure while the entire viscometer is at a high over all pressure. It was used to measure viscosities in the range from 10^7 to $10^{12}CP$[7]. Kobayashi and Nazashima measured the viscosities of pure 2.2.2- trifluoroethanol and its aqueous solution in the temperature range 273 to 453 K and pressures up to $40MPa$ with a closed circuit capillary viscometer[9]. At high- pressure capillary viscometer was designed and built by Kashulines to measure the viscosities of super critical carbon-dioxide containing several types of dissolved liquid solutes[10].

Rolling or Falling body Viscometer

Flowers is known as the first to point out and demonstrate the potential of rolling-ball Viscometer in 1914. Since then many attempts have been made to relate the viscosity of the fluid with the velocity of a rolling or falling body[12]. Bridgman is known to be the first to measure viscosity up to (1.2GPa) using falling-body viscometer. In his work, the velocity of falling mass was detected electronically and through an empirical equation the relative velocity was calculated. His viscometer consists of a cylinder into which the falling mass was placed, and then the whole system was in a pressure chamber. Scaling complexities and the need for very high pressure in order for the weight to fall were only a few limitation of this system. Later, Bridgman used improved high-pressure device where the entire pressure chamber was filled with the fluid under study, and only the fluid compatible with the components of the pressure chamber could be analyzed.

Stokes law which relates the viscosity of a Newtonian fluid to the velocity of a falling sphere is the principle of falling ball viscometers. If a sphere of radius of R and density, ρ_s, falls through a fluid of density ρ and viscosity η at a constant velocity v_t,

the following relationships holds

$$\eta = \frac{2(\rho_s - \rho)gR^2}{9v_t} \tag{2.1.4}$$

where g is the gravitational acceleration. With these viscometers, fall times should be measured when the ball reaches the terminal velocity. In rolling ball viscometers, similar to the falling ball viscometers, the speed of the rolling sphere down in a cylindrical tube include at a fixed angle to the horizontal is used to determine the viscosity. In this case the velocity, v_t, in the equation is the translational velocity of the rolling sphere.

Falling cylinder, or sinker, viscometers are used on the similar working principle to that of the falling ball viscometers. The only difference being the shape of the weight. Determination of the absolute viscosity requires the precise knowledge of the geometry of the cylinder and the force acting on it. Therefore most measurements are made relative to viscosity for Newtonian fluid is described by Lohrenz et al. in 1960 [5] as follows;

$$\eta = \frac{t(\rho_s - \rho)gr^2{}_1[(r_2^2 + r_1^2)\ln(\frac{r_2}{r_2}) - (r_2^2 - r_1^2)]}{2L(r_2^2 + r_1^2)} \tag{2.1.5}$$

where η is the viscosity, t is the falling time, ρ_s is the density of the sinker, and ρ_f is the density of the fluid , L is the vertical fall distance, r_1 and r_2 are the radius of the sinker and inner radius of the fall ball and tube respectively[5].

A rolling ball viscometer was constructed by Schmidt and Wolf which can be operated up to 4000 bar for the measurements of both dilute and concentrated polymer solutions [13]. They measured polystryrene or tert-butylacetate solution viscosities temperature up to 403K and pressures higher than 4000bars.

Sanishawiski and Luft developed a rolling ball viscometer, which consists of a gas

tube, closed at one end, with a steel ball inside [14]. Electromagnet was placed at the open end of the tube, and this arrangement was installed in a high pressure autoclave. Two pairs of measuring coils are used to detect the rolling ball inductively. This instrument was used at pressures up to 195MPa and temperatures up to 413K to measure the viscosity of alcohol-ethene mixtures by sulzner etal.[14].

In 1991, a falling-cylinder viscometer which can operate up to 473K and 70MPa was designed by Kuran and his coworker[5,15]. The viscometer consisted of a fall tube, a view cell and a variable volume attachment. Density measurement are based on the measurement of the inside volume of the viscometer and the knowledge of the mass of the sampled loaded. The viscosity measurements are based on the measurement of the fall time of a sinker falling vertically in a cylinderical tube. In this instrument a ferromagnetic 416 stainless steel sinker was used. Depending on the viscometer and experimental condition various falling or falling body types have been used for determination of viscosity. Sawamura et al. used a glass ball in their high- pressure rolling ball viscometers of non magnetic 316 stainless steel sinker with a density of $7.28\frac{gm}{cm^3}$ and small ferritecore embedded into is used at a high pressure self-centering falling-body viscometer by Mathotra et al.[17].

Vibrating-Wire Viscometers

Vibrating wire viscometer is an alternative method that makes use of the effect of the fluid on the oscillation of a body immersed in the fluid. The first vibrating-wire viscometer was developed in 1964 by Tough et al. Cylindrical wire was chosen as the most suitable geometry for high pressure operation[12,14]. The methods involves setting a thin tungsten wire into traversal vibration and determining the damping

of this motion by the surrounding sample liquid. The wire is set into vibration by means of Lorentz force generated by an alternating electrical current and a magnetic field raised by an electromagnet. After the current is stopped, the free damped oscillation of the wire in the magnetic field, sampled and stored on a computer disk. The damping of this signal is a measure for the viscosity of the sample fluid. In the working equation of vibrating wire, the viscosity and the density are coupled. But the sensitivity of density is in practice too low for precise determination of this property. Therefore, previous knowledge of the density of the fluid is necessary in order to determine its viscosity accurately.

In 1998, Padua et al. explored a new arrangement for the vibrating wire sensor in which the wire is tensioned by a suspended weight, or sinker. The density of the fluid is determined by hydrostatic weighing, with the wire acting as a force sensor. In 1997, Gulik extended the operation range of vibrating- wire viscometer by determining the viscosity of the liquid carbon dioxide below ambient temperatures, between 217K to 304K, and pressures up to 500MPa.

Assail et al.[12] described the design and operation of the vibrating- wire viscometer capable of measuring pressure up to 100MPa, based on the similar procedures santos and Castro followed. The advantage of vibrating-wire technique is that it does not require extensive calibration procedures, once the physical parameters of the sensor are determined (length, radius, Young's modules of the wire , volume and mass of the sensor), no additional calibrations are necessary for operation in different fluid or at condition away from room temperature and atmospheric pressure. The disadvantage is density cannot be determined along the viscosity in most of them, other techniques need to be explored for density calculation.

Capillary tube Viscometer

In this experiment the flow rate and pressure drop across a capillary tube are measured. As with the falling ball experiment, these measurements yield the shear rate and the velocity profile and thus can be used to determine the fluid viscosity. The capillary viscometry is based on the fully developed laminar tube flow theory (Hagen-Poiseuille flow) and is shown in ($Fig2.2$). The capillary tube length is many times larger than its diameter, so that entrance flow is neglected or accounted for in more accurate measurement or for shorter tubes. The expression for the shear stress τ at the wall is ;

$$\tau_\omega = [\frac{\triangle p}{L}][\frac{p}{4}] \tag{2.1.6}$$

and

$$\triangle p = (p_1 - p_2) + (z_1 - z_2) - [\frac{C\rho V^2}{2}] \tag{2.1.7}$$

where $C \approx 1.1$, p, z, $V = \frac{4Q}{\pi d^2}$, and Q are correction factor, pressure, elevation, the mean flow velocity, and the fluid volume flow rate, respectively. The subscript 1 and 2 refer to the inlet and outlet, respectively. The expression for the shear rate at wall is;

$$\frac{d\gamma}{dt} = [\frac{3n+1}{4n}][\frac{8U}{D}] \tag{2.1.8}$$

where $n = d\log[\frac{\tau_\omega}{d}](\log[\frac{8U}{D}])$ is the slop of the measured $\log(\tau_\omega) - \log(\frac{8U}{D})$ curve. Then ,the viscosity is simply calculated as ;

$$\eta = \frac{\tau_\omega}{\frac{d\gamma}{dt}} = [\frac{4n}{(3n+1)}][\frac{\triangle PD^2}{321U}] = [\frac{4n}{(3n+1)}][\frac{\Delta PD^4\Pi}{128QL}] \tag{2.1.9}$$

note that n=1, for a Newtonian fluid, so the first term, $[\frac{4n}{3n+1}]$ become unity and disappears from eq(2.1.9).

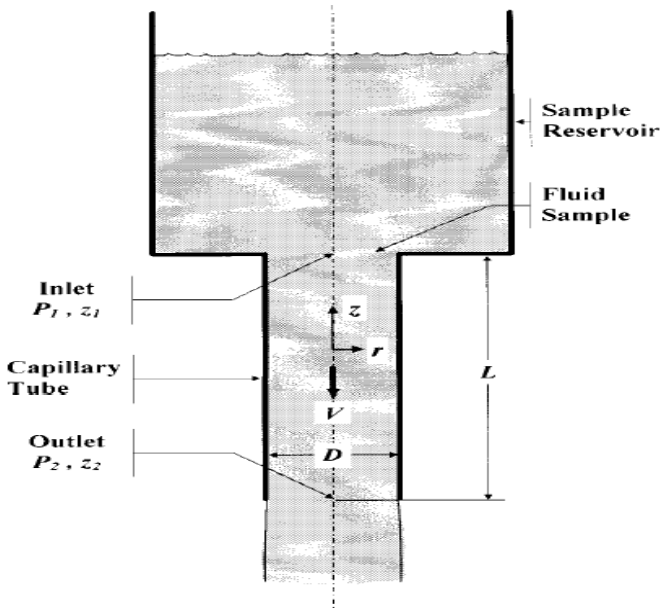

Figure 2.2: Capillary tube viscometer geometry

1. the advantage of capillary over rotational viscometer are low cost, high accuracy (particularly with larger tubes), and the ability to achieve very high shear rates, even with high viscosity samples

2. the main disadvantages are high residence time and variation of the shear across the flow, which can change the structure of complex test fluids, as well as shear heating with high viscosity samples.

Concentric Cylinders

Concentric cylinder type viscometer or rheometry are usually employed for absolute viscosity measurements, which requires a knowledge of well defined shear rate and shear stress data. Usually the torque on the stationary, cylinder and rotational velocity of the other cylinder are measured for determination of the shear stress and

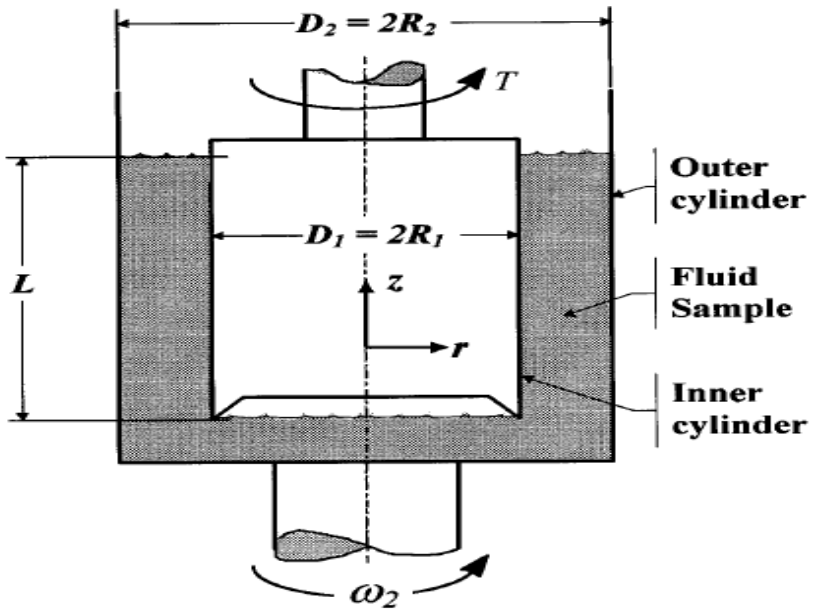

Figure 2.3: Concentric cylinder viscometer geometry

shear rate, which is needed for viscosity calculation. Once the torque, T, is measured, it is simple to describe the fluid shear stress $\tau_{r\theta}$ at any point with radius r between the two cylinders, as shown in $Fig2.3$.

$$\tau_{r\theta}(r) = [\frac{T}{2\pi r^2 L_e}] \tag{2.1.10}$$

where $L_e = (L + L_c)$, is the effective length of the cylinder at which the torque is measured. In addition to the cylinders length L, it takes into account the end-effect correction L_c. For narrow gab between the cylinder ($\beta = \frac{R_2}{R_1} \approx 1$), regardless of the fluid type, the velocity profile can be approximated as linear, and the shear rate with in the gap will be uniform:

$$\gamma(r) \approx [\frac{\Omega R}{R_2 - R_1}] \tag{2.1.11}$$

where $\Omega = (\omega_2 - \omega_1)$ is the relative rotational speed and $\bar{R} = (\frac{R_1+R_2}{2})$, is the mean radius of the inner(1) and outer(2) cylinders; actually, the shear rate profile across the gap between the cylinders depend on the relative rotational speed, radii and the fluid properties. However, there is a simpler procedure [10] that has been established by German standards[11].

For any fluid, including non-Newtonian fluids, there is a radius at which the shear rate is virtually independent of the fluid, type for a given Ω. This radius, being a function of geometry only, is called the representative radius, R_R, and is determined as the location corresponding to the so-called representative shear stress, $\tau_R = (\frac{\tau_1+\tau_2}{2})$, the average of the stresses at the outer and inner cylinder interfaces with the fluid, that is:

$$R_R = R_1[\sqrt{\frac{2\beta^2}{1+\beta^2}}] \tag{2.1.12}$$

Since the shear rate at the representative radius is virtually independent on the fluid type (whether Newtonian or non-Newtonian), the representative shear rate is simply calculated for Newtonian fluid ($n = 1$) and $r = R_R$, according to [10]:

$$\frac{d\gamma_R}{dt} = \frac{d\gamma_{r=R_R}}{dt} = \omega_2[\frac{\beta^2+1}{\beta^2-1}] \tag{2.1.13}$$

The accuracy of the representative parameter depends on the geometry of the cylinders β and fluid type n. It is shown in [10] that, for an unrealistically wide range of fluid type ($0.35 < n < 3.5$) and cylinder geometry ($\beta = 1 upto 1.2$), the maximum errors are less than 0.6 percent. Therefore, the error associated with the representative parameter concept is virtually negligible for practical measurements. Finally the (apparent) fluid viscosity is determined as the ratio between the shear

stress and corresponding shear rate using eq (2.1.5) to eq (2.1.8), as ;

$$\eta = \eta_R = \frac{\tau_R}{\frac{d\gamma_R}{dt}} = [\frac{\beta^2 - 1}{4\pi\beta^2 R_1^2 L_e}]\frac{T}{\omega_2} = [\frac{\beta^2 - 1}{4\pi R_1^2 L_e}]\frac{T}{\omega_2} \tag{2.1.14}$$

For a given cylinder geometry β, R_2, and L_e, the viscosity can be determined from eq(2.1.8) by measuring torque T and angular velocity ω_2. As already mentioned, in couette-type viscometry, the Taylor vortices with in the gap virtually eliminated. However, vortices at the bottom can be present, and their influence becomes important when the Reynolds number reaches the value of unity[10,11]. Furthermore, flow instability and turbulence will develop when the Reynolds numbers reaches values of 10^3 and 10^4. The Reynolds number R_e, for the flow between concentric cylinder is defined [11] as;

$$R_e = [\frac{\rho\omega_2 R_1^2}{2\eta}][\beta^2 - 1] \tag{2.1.15}$$

The main advantage of the rotational viscometer compared to many other viscometrs is its ability to operate continuously at a given shear rate, so that other steady state measurement can be conveniently performed. That way, time dependency if any, can be detected and determined. Also, subsequent measurements can be made with the same instrument and sampled at different shear rates, temperature, etc. For these and other reasons, rotational viscometers are among the most widely used class of instrument for rheological measurements.

Cone-and-plate viscometer

The simple cone-and plate viscometry geometry provides a uniform rate of shear and direct measurements of the first normal stress difference. It is the most popular instrument for measurement of the non-Newtonian fluid properties. The working

shear stress and shear strain rate equations can be easily derived in spherical coordinate, as indicated by the geometry in ($Fig2.4$), and are respectively.

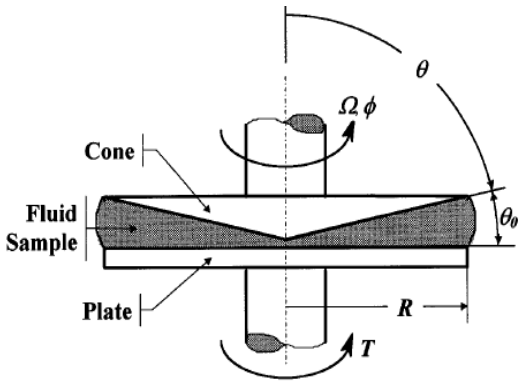

Figure 2.4: Cone- and plate- viscometer geometry

$$\tau_{\theta\phi} = [\frac{3T}{2\pi R^3}] \tag{2.1.16}$$

and

$$\frac{d\gamma}{dt} = \frac{\Omega}{\theta_0} \tag{2.1.17}$$

where, R and $\theta_0 < 0.1$ are the cone radius and angle, respectively. The viscosity is the easily calculated as;

$$\eta = \frac{\tau_{\theta\phi}}{\frac{d\tau}{dt}} = [\frac{3T\theta_0}{2\pi\Omega R^3}] \tag{2.1.18}$$

Inertial and secondary flow increase while shear heating decrease the measured torque T_m. The torque correction is given as;

$$\frac{T_m}{T} = 1 + 6 * 10^{-4} R_e^2 \tag{2.1.19}$$

where

$$R_e = \frac{\rho\Omega\theta_0 R}{\eta} \tag{2.1.20}$$

Parallel disks

This geometry Fig2.5, which consists of a disk rotating in a cylindrical cavity, is similar to the cone-and-plate geometry, and many instruments per unit the use of either one. However, the shear rate is so longer uniform,but depends on radial distance from the axis of rotation and on the gap h, that is;

$$\frac{d\gamma_r}{dt} = \frac{r\Omega}{h} \tag{2.1.21}$$

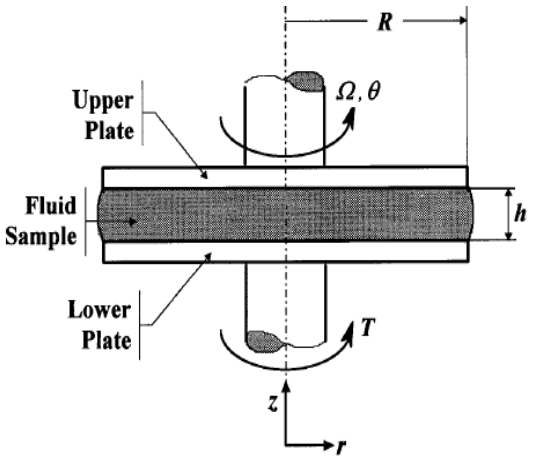

Figure 2.5: Parallel disk viscometer geometry

For Newtonian fluids after integration over the disk area, the torque can be expressed as a function of viscosity, so that the later can be determined as;

$$\eta = [\frac{2Th}{\pi\Omega R_4}] \tag{2.1.22}$$

Falling body method: Falling- cylinder

The falling cylinder method is similar in concepts to the falling sphere method except that a flat-ended, solid circular cylinder freely falls vertically in the direction of its longitudinal axis through a liquid sample with in a cylindrical, container. A schematic diagrams of the configuration is shown in $Fig2.6$. Taking an infinitely long-cylinder of density ρ_2 and radius r_c falling through a Newtonian fluid of density ρ_1 with infinite extent, the resulting shear viscosity of the fluid is given as;

$$\eta = \frac{g r_c^2 (\rho_2 - \rho_1)}{2U_{ter}} \tag{2.1.23}$$

Just as with the falling sphere, a finite container volume necessitates modifying, to the effect of container walls and ends. A correction for container wall effects can be analytically deduced by balancing the buoyancy and gravitational force on the cylinder, of length L, with the shear force on the sides and the compressional forces on the cylinder trailing end and the tensile force on the cylinder trailing end. The resulting correction terms, or geometrical factor, $G(k)(k = \frac{r_c}{r})$, depends on the cylinder radius, and the container radius, r and is given by;

$$G(k) = \frac{k^2(1 - \ln k) - (1 + \ln k)}{(1 + k^2)} \tag{2.1.24}$$

Unlike the fluid flow around a falling sphere, the fluid motion around a falling flat-ended cylinder is very complex. The effect of container ends are minimized by creating a small gap between the cylinder and container wall. If a long cylinder (here, a cylinder is considered long if $\psi \geq 10$, where $\psi = \frac{L}{r}$) with a radius nearly as large as the radius of the container is used, then the effects of the walls would dominate, thus by reducing the end effects to a second-order effects.

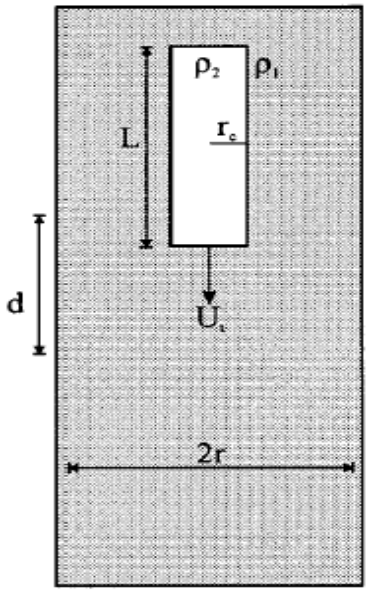

Figure 2.6: Schematic diagram of the falling cylinder viscometer

A major draw back with this approach is, however, if the cylinder and container are not concentric; the resulting inhomogeneous wall shear force would cause the downward motion of the cylinder to become eccentric. The potential for misalignment, motivated the recently obtained analytical solution to the fluid flow about the cylinder ends[16], an analytical expression for the end correction factor ECF was then deduced[17] and is given as;

$$\frac{1}{ECF} = 1 + [\frac{8k}{\pi C_\omega}][\frac{G(k)}{\psi}] \tag{2.1.25}$$

where $C_\omega = [1 - 0.003852 - 1.961019k + 0.9570952k^2]$, was derived semi-empirically[17] as a disk wall correction factor. This is based on the idea that the drag force on a disk eq(2.1.20) is valid for $\psi \leq 30$ and agrees with the empirically derived correction [16] to within 0.6 percent with wall and end effects taken into consideration. The

working formula to determine the shear viscosity of a Newtonian fluid from a falling cylinder viscometry is;

$$\eta = \frac{g r_c^2 (\rho_2 - \rho^1) G(k)}{\frac{2U_{ter}}{ECF}} \tag{2.1.26}$$

Falling sphere:

The falling sphere viscometry is one of the earliest and least involved methods to determine the absolute shear viscosity of a Newtonian fluid. In this method, a sphere is allowed to fall freely a measured distance through a viscous liquid medium and its viscosity is determined. The viscous drag of the falling sphere results in the creation of a restraining force, F, described by Stokes law;

$$F = 6\pi\eta r_s U_{ter} \tag{2.1.27}$$

where r_s is the radius of the sphere and U_{ter} is the terminal velocity of the falling body. If a sphere of density ρ_2 is falling through a fluid of density ρ_1 in a container of infinite extent, then by balancing eq(2.1.22) with the net force of gravity and buoyancy exerted on a solid sphere, the resulting equation of absolute viscosity is;

$$\eta = \frac{2g r_s^2 (\rho_2 - \rho_1)}{9U_{ter}} \tag{2.1.28}$$

This shows the relation between the viscosity of a fluid and terminal velocity of a sphere falling within it, having a fine container volume necessitates the modification of eq(2.1.23) to correct for effect on the velocity of the sphere due to interaction with container walls (ω) and ends (E).

Considering a cylindrical container of radius r and height H, the corrected forms of eq(2.1.23) can be written as ;

$$\eta = \frac{2g r_s^2 (\rho_2 - \rho_1)\omega}{9U_{ter}E} \tag{2.1.29}$$

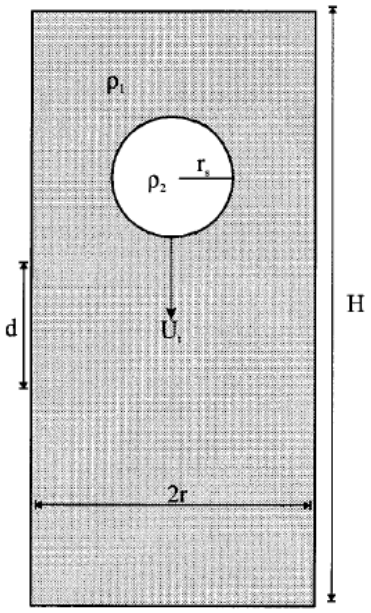

Figure 2.7: Schematic diagram of the falling sphere viscometer

where

$$\omega = [1 - 2.1044(\frac{r_s}{r}) + 2.09(\frac{r_s}{r})^3 - 0.95(\frac{r_s}{r})^5] \tag{2.1.30}$$

and

$$E = 1 + 3.3(\frac{r_s}{H}) \tag{2.1.31}$$

The wall correction was empirically derived[15] and is valid for $0.16 \leq (\frac{r_s}{H}) \leq 0.32$. Beyond this range, the effects of container walls significantly impair the terminal velocity of a sphere, thus giving rise to a false high viscosity, value.

2.2 Falling-sphere problem

Falling-sphere problem enjoys great attention from today scientists. The idea exists this simple experimental method (widely used to encounter the Newtonian

viscosity) could be used to measure the material properties on a simple and cheap basis. When a sphere falls, it initially accelerates under the action of gravity. The resistance to motion is due to the shearing of the liquid passing around it. At same point, the resistance balances the force of gravity and the sphere falls at a constant velocity(means, the difference between the consecutive falling velocity of a sphere might be very small). This is the terminal velocity.

For a body immersed in a liquid, the buoyancy weight is W and this is equal to the viscous resistance R when the terminal velocity is reached. The basic idea is a sphere is placed in the center line of a tube (Fig2.8). The sphere is suspended by using a fine steel wire(0.1mm). The assumption is made that wire does not have a large effect on the force and velocity of the sphere. The wire is champed above the sphere. The experiments, the sphere is monitored by a video system and the co-ordinate are measured.

The choice of the density of the sphere and the ratio (a/R) (resistance due to the tube boundary) defines the weissenberg number. This number is given by:

$$W_i = \frac{\theta U_{max}}{a} \tag{2.2.1}$$

where U_{max} is the maximum velocity (first over shoot). The Weissenberg number is important for the numerical solution. The higher the W_i the more difficult it is to obtain a convergent solution.

Recently Backer and Mckinley[9] have carried out this experiment. It was done with a polyisobutylene(PIB) Boger fluid. The over all experiment is shown in (Fig2.8). A long plexiglas cylinder is filled with Boger fluid. The entire cylinder is enclosed in a rectangular box filled with refractive index matched in a centered release-mechanism. In our case the principle of the problem is mentioned in subsection(2.3) and sphere

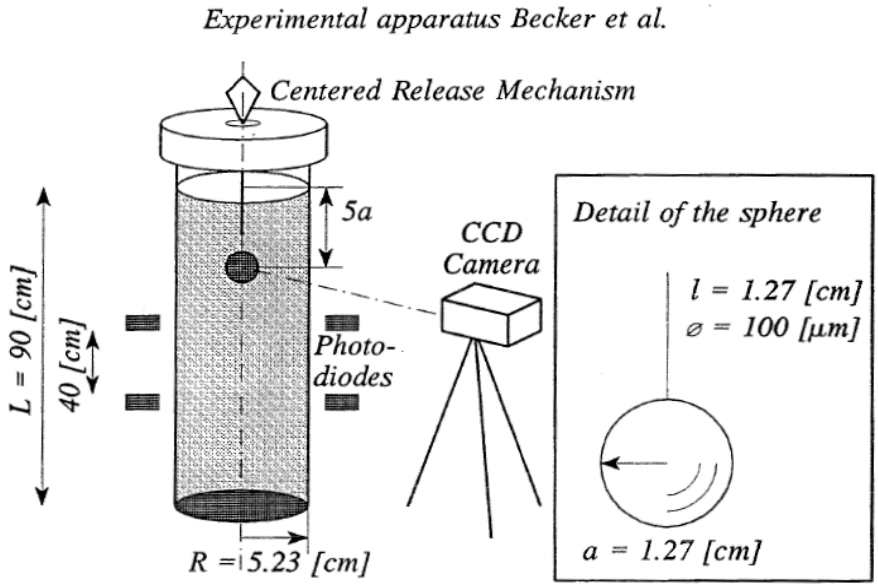

Figure 2.8: Schematic diagram of the experimental apparatus, used by Becker et al., for measuring transient and steady motion of a sphere falling through a viscoelastic fluid

release mechanism is briefly stated in chapter 3.

2.3 Principle of One-fluid model

As a ball falls under the effects of gravity in a cylindrical tube containing a Newtonian fluid the viscosity of the fluid is to be measured. The fundamental principle of dynamics is applied to the falling ball with the following external force: gravitational force, ($F_g = Vg\rho_b$) that pulls the ball down through the fluid, where V is volume of a sphere, Stokes drag force, ($F_D = -\frac{C_D}{2}\rho_f A u^2$) that resist that falling of the ball, where ρ_f - density of the fluid, C_D - drags coefficient, when the size of the container is comparable to the size of the ball, the effects of the container must be taken in to

account.

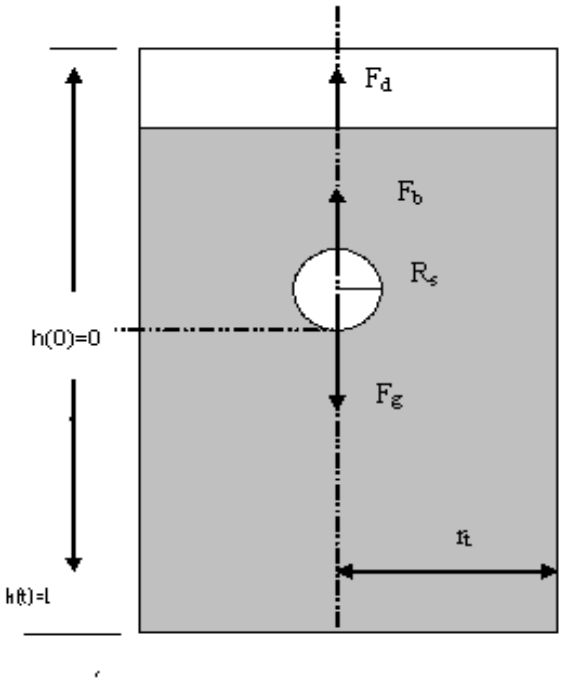

Figure 2.9: Schematic diagram of a ball falling through a single fluid

In order to establish the theoretical model for a ball falling through a single fluid (Fig2.9), we first sum the buoyancy and the drag force acting on the sphere;

$$F_{drag} = -\frac{C_D}{2}\rho_f A(\frac{dh}{dt})^2 \tag{2.3.1}$$

$$F_{buoyancy} = Vg[\rho_b - \rho_f] \tag{2.3.2}$$

Where C_D is the coefficient of drag A is cross sectional area of the sphere, h is the height of the sphere as a function of time t, ρ_f - is density of the fluid, ρ_b - is the density of the sphere, V ,- is the volume of the ball. Applying Newtons law in the

(Fig2.9), then it gives;

$$m_b \frac{d^2h}{dt^2} = F_D + [F_g - F_b] \tag{2.3.3}$$

substituting eq(2.3.1) and eq(2.3.2) into eq(2.3.3) yields;

$$m_b \frac{d^2h}{dt^2} = -\frac{C_D}{2}\rho_f A(\frac{dh}{dt})^2 + Vg[\rho_b - \rho_f] \tag{2.3.4}$$

Next, we non dimentionalize the governing equation eq (2.3.4). To do this, we scale both the time t and height h. as $H = \frac{h}{L}$, where L) is the total height of the fall, and $T = \frac{t}{\tau}$, where $\tau = \sqrt{\frac{m_b L_{TOT}}{Vg[\rho_b - \rho_f]}}$ -is a reasonable time scale that will be determined later. After differentiating h with respect to t and substituting into eq. 2.3.4 yields

$$m_b \frac{L}{\tau^2}\frac{d^2H}{dT^2} = -\frac{C_D}{2}\rho_f A(\frac{dH}{dT})^2 \frac{L}{\tau^2} + Vg[\rho_b - \rho_f] \tag{2.3.5}$$

This can be simplified by dividing both sides by $(\frac{m_b L}{\tau^2})$, and combining the constants into one non-dimensional constant ε.

$$\frac{d^2H}{dT^2} = -\varepsilon \frac{d^2H}{dT^2} + 1 \tag{2.3.6}$$

Where

$$\varepsilon = \frac{C_D \rho_f A L_{TOT}}{2m} \tag{2.3.7}$$

Since the initial non-dimensional height $H = 0$, and the initial velocity of the ball $\frac{dH}{dT}$, we have the initial condition: $H(0) = 0$, $\frac{dH}{dT}(0) = 0$. We know that when a sphere(ball) reaches a terminal velocity U_{ter}, the acceleration term $\frac{d^2H}{dT^2}$ is zero. Setting the right-hand side eq (2.3.5) equal to zero and solving for $\frac{dH}{dT}$ in terms of ε will give the non-dimensional terminal velocity,

$$\frac{dH}{dT} = \frac{1}{\sqrt{\varepsilon}} \tag{2.3.8}$$

Now we scale this non-dimensional terminal velocity by the scaling factor ($\frac{L_{TOT}}{\tau}$), giving us the dimensional terminal velocity;

$$\frac{dH}{dT} = \frac{1}{\sqrt{\varepsilon}} \frac{L_{TOT}}{\tau} \tag{2.3.9}$$

using ε from eq(2.3.7) and $\tau = \sqrt{\frac{m_b L_{TOT}}{Vg[\rho_b - \rho_f]}}$, the terminal velocity U_{term} will take the following form:

$$U_{term} = \sqrt{\frac{2Vg(\rho_b - \rho_f)}{C_D \rho_f A}} \tag{2.3.10}$$

For low Reynolds number, the stokes drag force on a spherical particle is given by;

$$F_D = 3\pi\eta U D_s \tag{2.3.11}$$

where U is relative velocity of the fluid with respect to the particle. By equating eq(2.3.11) with eq(2.3.1), we get a relation;

$$\frac{6\pi\eta(D_s)}{U} = C_D \rho_f A \tag{2.3.12}$$

Substituting eq(2.3.12) into eq(2.3.10), it yields;

$$\eta = [\frac{2Vg(\rho_s - \rho_f)}{6\pi(U_{t)D_s}}] \tag{2.3.13}$$

where $V = \frac{\pi(D_s)^3}{6}$

$$\eta = [\frac{(D_s)^2 g(\rho_s - \rho_f)}{18U_{ter}}] \tag{2.3.14}$$

Under the condition of the experiment, the terminal velocity will be less than the unbounded medium because the ball will experience the wall effects, the end effects and the inertial effects.

In order to determine the experimental terminal velocity; $U_{ter.Dim(=U_\infty)}$), we multiply the correction factor K_ω into eq(2.3.7). Therefore eq(2.3.14) becomes;

$$\eta = [\frac{(D_s)^2 g(\rho_s - \rho_f)}{18U_{corr}}] \tag{2.3.15}$$

Where η is dynamic viscosity of the fluid, then the corrected terminal velocity of a falling sphere can be expressed as;

$$U_{corr} = U_m K_\omega \tag{2.3.16}$$

where U_m , K_ω are measured values of a falling velocity and correction factor respectively. Then by eq(2.4.2), for very low Reynolds number eq(2.3.16) can be expressed as follows;

$$U_{corr} = U_m[1 - 2.1044(\frac{D_s}{D_t}) + 2.09(\frac{D_s}{D_t})^3 - 0.95(\frac{D_s}{D_t})^5]^{-1} \tag{2.3.17}$$

then eq(2.3.15) becomes

$$\eta = [\frac{(D_s)^2 g(\rho_s - \rho_f)}{18U_m}][1 - 2.1044(\frac{D_s}{D_t}) + 2.09(\frac{D_s}{D_t})^3 - 0.95(\frac{D_s}{D_t})^5] \tag{2.3.18}$$

2.4 Factor which affects on the terminal velocity of falling -sphere

In order to determine the experimental terminal velocity U_{term} a number of corrections must therefore be applied;

2.4.1 Correction factor due to wall/edge effects

The correction for the wall effects is given by the theoretical results obtained by Faxen [2], who resolved the momentum equation $\nabla^2 U = \frac{\triangle(p)}{\eta}(\triangle(U) = 0)$, where U is velocity and P- the pressure that applied to this problem with the reflection- methods. The analytical solution for a sphere of diameter D_s in translation with constant speed

U_{stokes} was developed by stokes [12] within the limit of R_e and in an infinite medium. In a finite field of diameter (cylindrical tube of diameter D_t field with oil), the effects caused by rigid wall involves an increase in the viscous dissipation which decreases the spheres speed [13]. The correction factor due to the wall attachments effects $K(\frac{D_s}{D_t})$ for creeping flow of a Newtonian fluids will decrease in the speed resulting from the presence of the wall as a function from the ratio of the rays between those of the sphere and the tube ($\frac{D_s}{D_t}$). It is defined in experiments by;

$$K(\frac{D_s}{D_t}) = [\frac{U_{stokes}}{U_\infty(\frac{D_s}{D_t})}] \tag{2.4.1}$$

The drag forces can thus be defined by $3\pi\eta U_\infty K_\omega$.

Faxen[14] solved the equation of the motion while taking into account the boundary condition simulating the wall and by using the approximation of Oseen[5], he obtained a coefficient of correction applied to the stokes force for a sphere falling into a cylinder:

$$\frac{F}{F_\infty} = [1 - \frac{3}{16}R_e - \frac{D_s}{D_t}f(\frac{R_e}{4}\frac{D_s}{D_t}) + 2.09(\frac{D_s}{D_t})^3 - 0.95(\frac{D_s}{D_t})^5 + ...]^{-1} \tag{2.4.2}$$

Where the function f has the following value: $f(0) = 2.104$; $f(0.5) = 1.76$; $f(1) = 1.48$; $f(2) = 1.04$; $f(5) = 0.46$.

Bohlin[15], in a theoretical study using an extensions of Faxens reflection-method obtained the following correction, for $R_e \ll 1$ and $(\frac{D_s}{D_t}) < 0.6$;

$$K_P = [1-2.10443(\frac{D_s}{D_t})+2.08877(\frac{D_s}{D_t})^3-0.94813(\frac{D_s}{D_t})^5-1.372(\frac{D_s}{D_t})^6+3.87(\frac{D_s}{D_t})^8-4.19(\frac{D_s}{D_t})^{10}]^{-1} \tag{2.4.3}$$

In an experimental study: Francis [16] gave for $\frac{D_s}{D_t} < 0.97$ and $R_e < 1$;

$$K_P = [\frac{1 - 0.475(\frac{D_s}{D_t})}{1 - \frac{D_s}{D_t}}]^4 \tag{2.4.4}$$

Habberman and Sayre [17] also determined in experiments the coefficient K for $(\frac{D_s}{D_t}) < 0.8$ and $R_e \ll 2$:

$$K_P = [\frac{1 - 0.758557(\frac{D_s}{D_t})^5}{1 - 2.1050(\frac{D_s}{D_t}) + 2.086(\frac{D_s}{D_t})^3 - 1.7068(\frac{D_s}{D_t})^5 + 0.72603(\frac{D_s}{D_t})^6}] \tag{2.4.5}$$

Faxens formula was confirmed in experiments by Kawata[18], who, expressed the wall effects, for $(\frac{D_s}{D_t}) < 0.07$ and $R_e \ll 1$ by;

$$K_P = [1 - a_\omega(\frac{D_s}{D_t})]^{-1} \tag{2.4.6}$$

The a_ω function has the following values:a_ω =2.104 for $D_s = 2.0mm$ a_ω =2.103 for $D_s = 2.4mm$ a_ω =2.1099 for $D_s = 3.2mm$

Sutterby [19] also carried out experimental works on the wall and inertia effects for $0 < \frac{D_s}{D_t} < 0.13$ and $0.0001 < R_e < 3.78$. As a result, an empirical correction for the wall correction factor; $K_P = f(\frac{R_e D_t}{4D_s})$

2.4.2 Correction factor due to the inertial effects

A Reynolds number is defined based on the diameter of the ball;

$$R_e = \frac{\rho U_\infty d}{\eta} \tag{2.4.7}$$

When the inertial effects are negligible, the drag coefficient is written for $R_e \ll 1$;

$$C_D = \frac{24}{R_e} \tag{2.4.8}$$

Oseen[5], extended the stokes low by considering the fluid-inertia for $0 < R_e < 1$;

$$C_D = \frac{24}{R_e}(1 + \frac{3R_e}{16}) \tag{2.4.9}$$

This formula was improved by Proudman and Pearson[6], then by Ockendon and Ewans[7], who respectively obtained terms of higher degrees;

$$C_D = \frac{24}{R_e} = [1 + \frac{3R_e}{16} + \frac{9}{160}R_e^2 \ln(\frac{R_e}{2}) + \frac{0.1890}{4}_{R_e^2} + ...] \tag{2.4.10}$$

then

$$K_P = [1 + \frac{3R_e}{16} + \frac{9}{160}R_e^2 \ln(\frac{R_e}{2}) + \frac{0.1890}{4}_{R_e^2} + ...] \tag{2.4.11}$$

The correction factor to the fall velocity U as a function of Reynolds number R_e due to the inertial effect was reported by different researcher. Oseens [5] approximation of the Navier-stokes equation gives the following

$$U_{corr} = U_m[1 + \frac{3R_e}{16}]^{-1} \tag{2.4.12}$$

where R_e - is the Reynolds number. Goldstein[6] were derived the correction due to the higher order[6] as

$$U_{corr} = U_m[1 + \frac{3}{16}R_e - \frac{19}{128}R_e^2 + \frac{71}{20480}R_e^3 + ...]^{-1} \tag{2.4.13}$$

proudman and pearson[7] as;

$$U_{corr} = U_m[1 + \frac{3R_e}{16} + \frac{9}{160}R_e^2 \ln(\frac{R_e}{2}) + ...] \tag{2.4.14}$$

2.4.3 Correction factor due to end effects

The end effects were theoretically studied by Lorentz, in a length L tube, without considering the wall effect modeled later by Faxen[14]. For a sphere approaching a rigid infinite plane, he obtained the following correction;

$$K_b = 1 + \frac{9}{8}\frac{d}{2Z} \tag{2.4.15}$$

Where Z is the distance between the sphere and the cylinder base.

Tanner[22], reusing the methods of reflection taking into account the wall effect, modeled the end effects, and studied its influence on the total drag ($R_e \ll 1$). He gave the increases in the drag due to end effects according to the $\frac{2Z}{D_t}$ ratio where Z is the distance between the ball and the cylinder base and D_t the tube diameter.

For Sutterby [19], the correction due to the end effects is useless for; ($\frac{L}{D_t} > 2$), $R_e < 2$, $\frac{D_s}{D_t} < 0.125$. Works of Flude and Daborn[4] confirms the results obtained by Sutterby[19]. Indeed, it is not necessary to apply at the same time the correction due to the end effects and correction due to the edge effects, except if the ball is only a few diameters away from the tube base.

Chapter 3

Description of the experiment

3.1 Principle

The aim of our experiment is to obtain the viscosity of a given fluid by measuring the terminal velocity of a solid-sphere falling vertically under the influence of gravity in oil initially at rest (Fig3.1). The solid sphere is released without any initial velocity or rotation. The velocity of falling sphere is obtained using new acoustic method. It is based on the measurement of the position-time data for each sphere from video-movie motion of the sphere.

3.2 Apparatus and Procedure of the Experiment

3.2.1 Introduction

The experiment were designed to investigate the falling velocity field around a solid sphere accelerating from rest to terminal velocity between parallel wall which are performed in a long cylindrical transparent tube, filled with appropriate Newtonian viscous liquid. The observation were carried out using the high-speed camera, by capturing the motion of the sphere inside the tube during the fall. The following

section, describes the various components of the apparatus and sphere release mechanizm, which includes, the test tube, the digital CCD camera, the test fluid, the solid sphere, DC-light source, GERYK VACUUM PUMP.

3.2.2 Test tube

The experiment were conducted in a transparent glass of cylindrical tube with 135 cm long and 3.25 cm inner diameter. The tube was filled with Total quartz 20W50 motor oil, which allowed the viscosity of the mixture to be controlled. The viscosity of the fluid and the spacing between the walls are independent variables. Altering the viscosity changes the terminal velocity of the falling sphere and also the terminal Reynolds number achieved.

3.2.3 Test Sphere

The solid sphere is made of plastic and ranges in diameter from (1.232cm) to (1.336)cm. The sphere was initially submerged near the top of the tube from a vacuum pump release mechanism as shown in Fig3.1. The properties of the sphere are given in Table1.

sphere	diameter(cm)	mass(gm)	density($\frac{gm}{cm_3}$)
1	1.252	2.75	2.6767
2	1.336	3.05	2.4427
3	1.306	2.89	2.4779

Table1: Measured parameter of Test sphere

3.2.4 Sphere release Mechanism

The sphere was initially submerged and held in place near the top of the tube by vacuum pump method. The traversing rails allowed the sphere release mechanism to be positioned mid way between the parallel plane wall. The sphere are maintained by suction at the tip of a small tube in which a lower pressure is imposed by vacuum pump. The devices allows us to release the sphere at a given time just under the liquid surface (if any) in order to avoid air entrainment (no significant rotation has been observed with these devices when releasing the sphere).

3.2.5 CCD camera and recording optics

The recording medium used in this experiment was a full- frame interline transfer CCD in a power shot A550 canon digital camera, with a resolution of 7.1 MEGA PIXELS and can record at a speed of up to 60 frame per second. A charge-coupled device(CCD) consists of an array of charge-storage elements, a transport mechanism and an out put device, first introduced in 1969. A basic CCD consists of a series of closely spaced metal-oxide semi-conductor capacitor(MOS), each one corresponding to a single image pixel. In its most basic forms a CCD is a charge storage and transport devices and charge is stored on the MOS capacitors for read out and subsequent transformation to a digital image. More specifically, when a positive voltage, V, is applied to the surface of a P-type MOS capacitor, positive charge is called the depletion region. When a photon (i.e. light) enters the depletion region the electron released are stored in this region.

The charge-storage elements are either arranged linearly (the line-scan CCD), or arranged in a matrix structure (the area CCD). Each elements can transform the radiant energy incident on its surface in to an electrical charge. Underneath each

elements to the out put terminal of the device.

3.3 Experimental Set-Up

The experiment is performed in a cylindrical transparent tube of length about 135cm and inner diameter of 3.25cm, filled with Newtonian viscous fluid at rest in order to contain the fluid in a vertical position (Fig3.1). In this experiment 2-piece of 12V 100/90W DC-light is used as a source of light, high-speed video camera (power shot A550 canon CCD camera) is used to record the motion of the sphere inside the tube. It has a resolution up to 7.1MEGA PIXEL can record at speed of up to 60 frame per seconds. Three small sphere, made of plastic are used to measure the terminal velocity. The diameters of the sphere and the cylinder, screw gauge or micrometer, vernier caliper, and meter sticks are used to measure height of the tube, and weight of each sphere is measured using a CENT-GRAM balance 311g capacity.

3.4 Experimental Procedure

The experimental set up as show in (Fig3.1). The experimental set up is used to measure the velocity of the sphere moving in a fluid along the direction shown in Fig3.1. CCD camera was placed approximately 65cm from the cylinder and a piece of white cardboard was placed directly behind the cylinder to increase the contrast of the image. The entire motion of dropped sphere is recorded, and it is connected with a PC to generate the video in to image sequence frame by frame for each sphere in order to get position-time data of a falling sphere. Time was recorded in (1/60) of second, while distance was recorded in pixel per frame.

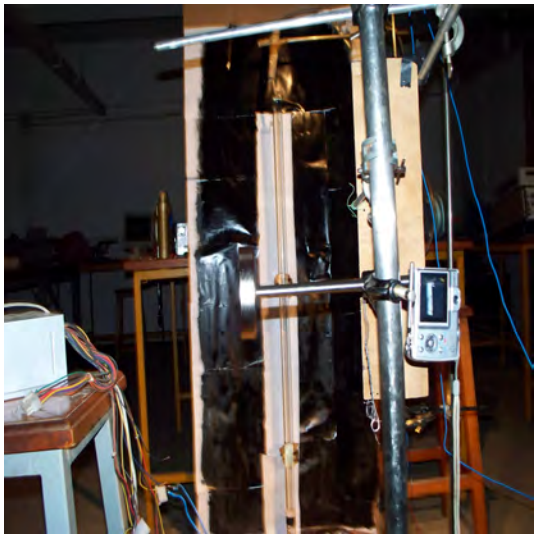

Figure 3.1: Diagram of experimental set up

The tube which contains the fluid 135 cm long with internal diameter 3.25 cm and its made of glass data has been collected for the falling velocities of a single sphere in Newtonian liquids using plastic beads of different diameters of the sphere are shown in Table1. We used a digital camera recorder to record the drop and played back the video frame by frame to obtain distance versus time data. Measuring the cylinder height with a ruler gave us a conversion factor from pixel to meter. All measurement were done at room temperature of 21 ^oC .

The solid sphere are carefully dropped using vacuum pump methods, in the center of the column and just below the liquid surface. From the measurement, we compute an average falling velocity and a standard deviation for each combination sphere solution using the average velocities so determined and the solid- liquid principle, we estimate the parameters of interest.

Chapter 4

Result and Discussion

4.1 Experimental Data

In the experiment, first, the average velocity of a sphere moving in Total quartz 20W50 motor oil at room temperature was calculated from the x-position of a sphere in [pixel] versus time [sec] data. Three spheres, sphere1, sphere2, and sphere3 of radius 0.626 cm, 0.668 cm, and 0.653 cm, were used and for each sphere 41 reading were recorded for total of 756 frame.

The data for determination of viscosity of Total quartz 20W50 motor oil for preliminary experiment by using sphere 1, sphere 2, and sphere 3 recording in Table 2, Table 3 and Table 4 respectively. Each data is taken within 18 frame intervals. Bearing ball made of plastic were dropped into transparent cylinders containing Total quartz 20W50 motor oil.

x[pixel]	2	42	80	124	163	206
	8	49	86	130	168	210
	15	54	91	136	173	215
	21	58	100	141	179	222
	25	62	104	147	188	227
	32	70	111	152	194	230
	36	76	120	158	200	
y[pixel]	4	7	6	8	6	6
	7	7	6	8	7	6
	6	5	5	6	6	5
	6	7	6	6	6	4
	7	8	6	7	6	6
	6	6	6	6	7	5
	7	6	6	6	6	
Time[sec]	0.3001	2.4007	4.5015	6.6022	8.7029	11.4038
	0.6002	2.7009	4.8016	6.6022	9.003	11.7039
	0.9003	3.001	5.1017	7.2024	9.3031	12.004
	1.2004	3.3011	5.4018	7.5025	9.6032	12.3041
	1.5005	3.6012	5.7019	7.8026	9.9033	12.6042
	1.8006	3.9013	6.002	8.1027	10.2034	12.9043
	2.1007	4.2014	6.3021	8.4028	11.1037	

Table 2: Measured values of x[pixel]- and y[pixel]- coordinate position pixel value and time[sec] for the sphere1 with diameter(d=1.252cm) in oil, scale=1.966$\frac{pixel}{cm}$

x[pixel]	3	50	89	131	16	202
	7	55	92	131	170	208
	13	61	97	141	176	213
	20	66	105	145	181	218
	28	72	109	150	188	224
	37	78	117	155	195	229
	44	85	122	159	196	
y[pixel]	4	7	6	7	6	5
	8	7	6	6	6	6
	8	6	6	6	6	7
	8	6	8	7	4	4
	8	7	7	5	7	6
	7	7	6	7	5	7
	6	7	6	5	6	
Time[sec]	0.3001	2.4007	4.5015	6.6022	8.7029	11.4038
	0.6002	2.7009	4.8016	6.6022	9.003	11.7039
	0.9003	3.001	5.1017	7.2024	9.3031	12.004
	1.2004	3.3011	5.4018	7.5025	9.6032	12.3041
	1.5005	3.6012	5.7019	7.8026	9.9033	12.6042
	1.8006	3.9013	6.002	8.1027	10.2034	12.9043
	2.1007	4.2014	6.3021	8.4028	11.1037	

Table 3: Measured values of x[pixel]- and y[pixel]- coordinate position pixel value and time[sec] for sphere 2 with diameter(d=1.336cm) in oil, scale=1.957$\frac{pixel}{cm}$

	3	44	89	128	167	206
	8	49	98	132	171	209
x[pixel]	15	59	102	138	177	211
	23	63	105	145	182	216
	28	69	110	151	187	221
	34	78	115	156	191	228
	40	83	122	160	196	
	3	8	8	7	7	6
	8	8	7	7	7	8
y[pixel]	8	8	7	8	6	6
	7	7	8	6	8	6
	8	8	7	6	6	7
	7	7	6	7	6	6
	8	8	6	6	7	
	0.3001	2.4007	4.5015	6.6022	8.7029	11.4038
	0.6002	2.7009	4.8016	6.6022	9.003	11.7039
	0.9003	3.001	5.1017	7.2024	9.3031	12.004
Time[sec]	1.2004	3.3011	5.4018	7.5025	9.6032	12.3041
	1.5005	3.6012	5.7019	7.8026	9.9033	12.6042
	1.8006	3.9013	6.002	8.1027	10.2034	12.9043
	2.1007	4.2014	6.3021	8.4028	11.1037	

Table 4: Measured values of x[pixel]- and y[pixel]- coordinate position pixel value and time[sec] for sphere 3 with diameter(d=1.306cm) in oil, scale=1.966$\frac{pixel}{cm}$

4.2 Data Analysis and Result

The images of the falling spheres were captured at 60 frame per second. Images were imported into image processing software image J, and the x-and y-coordinates of the sphere in each frame were determined by clicking on the center of the sphere

using Image J's built- in measurement tool (cross hair). Images were calibrated for length by imaging a ruler at the same location of the falling spheres. The sphere's position data were imported in to MATLAB and converted to position versus time.

The image was analysed in public domain image processing program, Image J, and calculation and plotting graph were done using MATLAB code. The average and standard deviation of the terminal velocity was calculated for each sphere size. Velocities of various sphere were calculated from Table 2, Table 3, and Table 4 are given in Table 5, Table 6, and Table 7 respectively.

Velocity[cm/sec]	3.3910	8.9013	9.0426	9.5564	9.5298	9.7020
	6.7820	9.2310	9.1133	9.5832	9.4947	9.6231
	8.4774	9.1556	9.0759	9.6078	9.4619	9.5929
	8.9013	8.9399	9.4194	9.5626	9.4841	9.6513
	8.4774	8.7600	9.2806	9.5860	9.6592	9.6219
	9.0426	9.1296	9.4100	9.5450	9.6743	9.5113
	8.7197	9.2041	9.6885	9.5674	9.6885	

Table 5: Calculated velocities [cm/sec] from Table [2] for a sphere of radius 0.626 cm and density $2.6767 \frac{gm}{cm^3}$

Velocity[cm/sec]	5.1099	10.6455	10.1062	10.1423	9.6324	9.5573
	5.9615	10.4090	9.7939	9.7013	9.6520	9.5752
	7.3809	10.3901	9.7188	10.0068	9.6703	9.5474
	8.5164	10.2197	9.9358	9.8791	9.6342	9.5209
	9.5384	10.2197	9.7715	9.8267	9.7036	9.5384
	10.5036	10.2197	9.9642	9.7781	9.7689	9.5135
	10.7064	10.3414	9.8953	9.6722	9.5384	

Table 6: Calculated velocities [cm/sec] from Table [3] for a sphere of radius 0.668 cm and density $2.4427 \frac{gm}{cm^3}$

	5.0865	9.3252	9.3817	9.4023	9.3544	9.2310
	6.7820	9.2310	9.4312	9.4358	9.4382	9.4398
Velocity[cm/sec]	8.4774	10.0034	9.7740	9.3252	9.3525	9.3252
	9.7491	9.7105	9.6078	9.3591	9.3782	9.1730
	9.4947	9.7491	9.3698	9.4556	9.3509	9.1556
	9.6078	9.6513	9.3252	9.4822	9.3252	9.1391
	9.6885	9.4463	9.2848	9.4463	9.2525	

Table 7: Calculated velocities [cm/sec]from Table [4]for sphere of radius 0.653 cm and density $2.4779\frac{gm}{cm^3}$

The x-coordinate of a sphere in [pixel] versus time [sec] graph of sphere of radius 0.626 cm, 0.668 cm, and 0.653 cm, in Total quartz 20W50 motor oil, is obtained from Table [2], Table [3], and Table [4] are show below in Fig4.1. Similarly, the falling velocity[cm/sec] versus time [sec] graph of sphere1, 2, and 3 in Total quartz 20W50 motor oil is obtained from Table [6], Table [7], and Table [8] are shown below in Fig4.2 and the measured terminal velocity of a falling sphere versus of time is fitted with the theoretical terminal velocity as a function of time are shown below in Fig4.3.

Now using the following results are obtained by inserting data in to eq(2.3.17). Therefore, the average falling velocities for various spheres without correction factor is obtained $9.1182cm/sec$, $9.5904cm/sec$, and $9.2439cm/sec$, and its standard deviation is 1.0548, 1.0839, and 0.8174 for sphere 1, sphere 2, and sphere 3 respectively. Thus, the average falling terminal velocity for three spheres is obtained

$$U_m = (9.3175 \pm 0.0165)\frac{cm}{sec} \tag{4.2.1}$$

But the corrected terminal velocity due to correction factor for sphere 1, sphere 2, and sphere 3 as calculated by eq(2.3.17) is $30.3188\frac{cm}{sec}$, $35.6573\frac{cm}{sec}$, and $33.0114\frac{cm}{sec}$, and

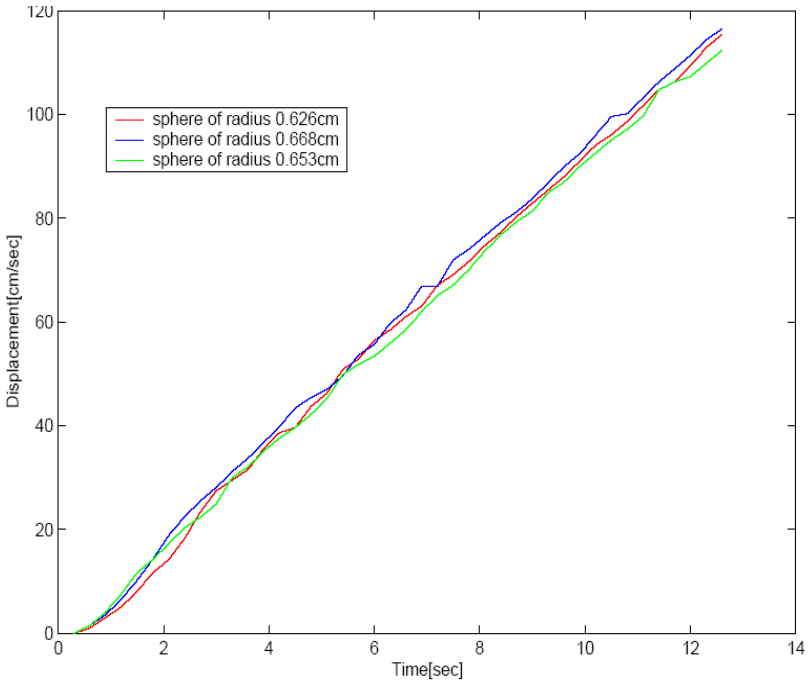

Figure 4.1: Displacement[cm] versus Time[sec] graph for a sphere1, sphere 2, and sphere 3 moving in Total quartz 20W50 motor oil

its standard deviation error are obtained as, 0.0095, 0.0126, and 0.0098 respectively. Thus corrected terminal velocity with its propagated standard uncertainty can be written as,

$$\begin{aligned} U1_{corr} &= (30.3188 \pm 0.0095)\frac{cm}{sec} \\ U2_{corr} &= (35.6573 \pm 0.0126)\frac{cm}{sec} \\ U3_{corr} &= (33.0114 \pm 0.0098)\frac{cm}{sec} \end{aligned} \tag{4.2.2}$$

Thus, the average corrected terminal velocity for three spheres is obtained

$$U_{corr} = (32.9958 \pm 0.01063) cm/sec$$

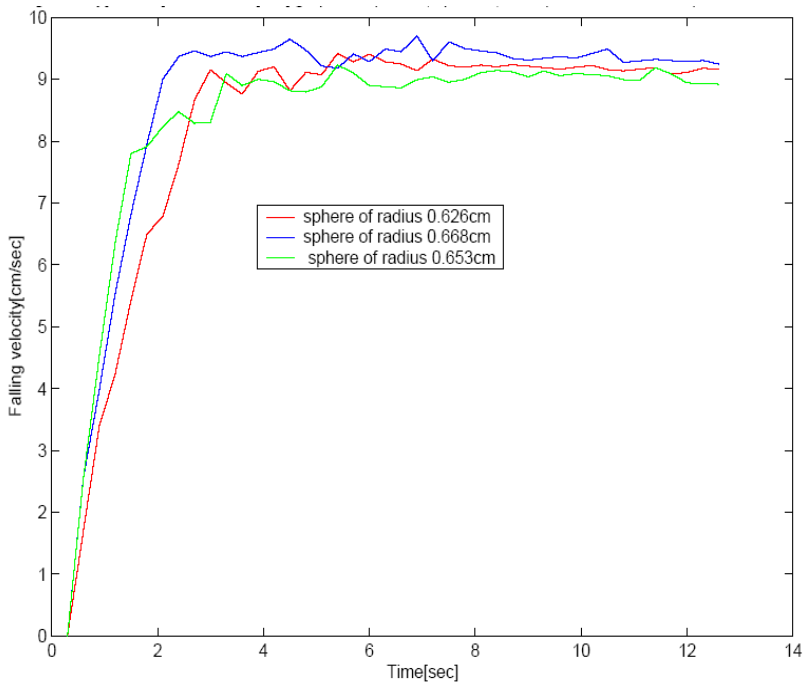

Figure 4.2: Falling velocity[cm/sec] versus Time[sec] graph for sphere 1, sphere 2, and sphere 3 falling in Total quartz 20W50 motor oil

Finally the dynamic viscosity of Total quartz 20W50 motor oil at room temperature with out correction factor as determined by sphere 1 is $\eta_1 = (3.3894 \pm 0.2120) centipoise$, and by sphere 2 is $\eta_2 = (3.4458 \pm 0..3021) centipoise$ and by sphere 3 is $\eta_3 = (3.3619 \pm 0.2011) centipoise$ respectively. Therefore, the average dynamic viscosity as calculated by eq(2.3.14) is

$$\eta = (3.3910 \pm 0.2384) centipoise \tag{4.2.3}$$

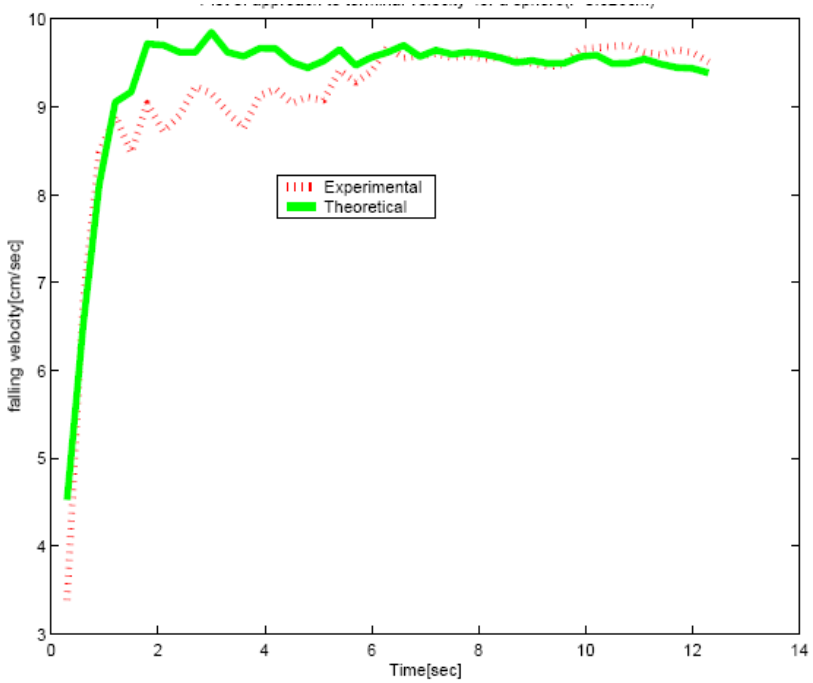

Figure 4.3: Plot of falling velocity approach to terminal velocity[cm/sec] versus of time[sec] for a sphere of radius(r=0.626cm) in oil the function use for fitting with measured falling velocity $U(t) = U_{ter}[1 - exp\frac{-t}{\tau}]$ is theoretical terminal velocity

But, the viscosity of Total quartz 20W50 motor oil at room temperature due to correction factor as determined by sphere1 is $\eta_1 = (4.6200 \pm 0.00885)centipoise$, and by sphere 2 is $\eta_2 = (5.3753 \pm 0.00738)centipoise$ and by sphere 3 is $\eta_3 = (4.8635 \pm 0.00773)centipoise$ respectively. Thus, the average dynamics viscosity of Total quartz 20W50 motor oil in this research is:

$$\eta = (4.9529 \pm 0.00799)centipoise \tag{4.2.4}$$

Therefore, dynamic viscosity as calculated by eq(2.3.18) is $\eta_{exp} = 4.9529centipoise$.

The dynamic viscosity of oil used in the experiment as measured with standard capillary viscometer at Total lubricant laboratory, is 4.987 centipoise. Finally, the percentage error of the dynamic viscosities can be computed by comparing with the values obtained with standard capillary viscometer. The average value obtained in the experiment is $\eta = (4.9529 \pm 0.00799)centipoise$, so that the value deviates by 0.688 percent from the reported value.

So we can say that the result of the experiment is satisfactory.

Chapter 5

Conclusion

In this thesis the expression for calculating the viscosity of liquid using Falling-sphere viscometer including a correction factor is presented. Falling-sphere viscometer requires, all correction factors which affects to the terminal velocity of the spheres that depend on the ratio of the diameters of the sphere to that of a cylinder and correction factor for the drag coefficient which depends on the Reynolds number are included in the expression. The viscosity of Total quartz 20W50 motor oil calculated using the expression of viscosity which is presented in this research is in good agreement with the reported value made by standard capillary viscometer.

5.1 Recommendation

In constructing Falling-sphere viscometer, only the motion of a spheres is considered including all factors which affected on the motion of a sphere. But, in reality as a sphere, is moving down, the fluid just below the sphere is displaced and accelerated in the upwards direction from rest. Because the motion of the sphere is the cause of motion of fluid. Therefore, there are portion of fluids, radial, vertical, and rotating component of fluids and at rest.

To construct a better viscometer, we should have to include the motion of fluid, and video of falling sphere in fluid should be captured using high resolution fast CCD camera can record at a speed of up to 500frame per second to get good data of position and time.

Appendix A

Error Analysis

In this work there are a number of a precision error in measurement of radius of cylinder, and sphere, density of the test fluid, and sphere , and mass of the sphere. The diameter of the cylinder are measured by vernier caliper and diameter of the sphere are measured by micrometer. The error arise in fraction of millimeters. Expected error as $(measuredvalue \pm 0.0025)$cm , radius of the cylinder r_c (1.625 ± 0.0025)cm, density of fluid(oil) $(= 0.893 \pm 0.0005)\frac{gm}{cm^3}$. These errors can propagate and calculated by using the following three rules:

Rule1: Multiplication and Division

If $z = x * y$ or $z = \frac{x}{y}$ then $\frac{\Delta z}{z} = Quadrature[\frac{\Delta x}{x}, \frac{\Delta y}{y}]$

In words, the fractional error in z is the quadrature of the fractional errors in x and y.

Rule2: Addition and Subtraction

If $z = x + y$ or $z = x - y$ then $\Delta z = Quadrature[\Delta x, \Delta y]$

In words, the error in z is the quadrature of the errors in x and y.

Rule3: Raising to a power

If $z = x^n$ then $\Delta z = nx^{(n-1)}\Delta x$ or equivalently $\frac{\Delta z}{z} = n\frac{\Delta x}{x}$

Calculated value are;

$$
\begin{aligned}
d_1 &= (1.252 \pm 0.001917)cm \\
d_2 &= (1.336 \pm 0.001871)cm \\
d_3 &= (1.306 \pm 0.001914)cm \\
D_t &= (3.25 \pm 0.000769)cm \\
\rho_1 &= (2.4427 \pm 0.000187)\frac{gm}{cm_3} \\
\rho_2 &= (2.4779 \pm 0.000205)\frac{gm}{cm_3} \\
\rho_3 &= (2.4779 \pm 0.0002020)\frac{gm}{cm_3} \\
\rho_f &= (0.893 \pm 0.00025)\frac{gm}{cm_3} \\
U_1 &= (9.1182 \pm 0.01810)\frac{cm}{sec} \\
U_2 &= (9.5904 \pm 0.01760)\frac{cm}{sec} \\
U_3 &= (9.2439 \pm 0.01380)\frac{cm}{sec} \\
g &= (0.981 \pm 0.0981)\frac{cm}{sec^2} \\
m_1 &= (2.75 \pm 0.000182)gm \\
m_2 &= (3.05 \pm 0.000164)gm \\
m_3 &= (2.89 \pm 0.000173)gm \\
t &= (6.3000 \pm 0.5612)sec \\
U1_{corr} &= (30.3188 \pm 0.000313)\frac{cm}{sec} \\
U2_{corr} &= (35.6573 \pm 0.000353)\frac{cm}{sec} \\
U3_{corr} &= (33.0114 \pm 0.000297)\frac{cm}{sec}
\end{aligned}
$$

Uncertainties calculation on the measurement system

The interest of this study being primarily metrologicaly, it is important to determine uncertainty on the terminal velocity measurement system. Therefore, the expression of the corrected terminal velocity and viscosity variance, $u^2(U_{corr})$, $u^2(\eta)$ respectively, by taking into account eq(2.3.17) and eq(2.3.18) becomes;

$$u^2(U_{corr}) = [\frac{\partial U_{corr}}{\partial U_m}]^2 u^2(U_m) + [\frac{\partial U_{corr}}{\partial D_s}]^2 u^2(D_s) + [\frac{\partial U_{corr}}{\partial D_t}]^2 u^2(D_t) \quad (5.1.1)$$

$$\begin{aligned} u^2(\eta) = {} & [\frac{\partial \eta}{\partial D_s}]^2 u^2(D_s) + [\frac{\partial \eta}{\partial D_t}]^2 u^2(D_t) + [\frac{\partial \eta}{\partial \rho_s}]^2 u^2(\rho_s) + \\ & [\frac{\partial \eta}{\partial \rho_f}]^2 u^2(\rho_f) + [\frac{\partial \eta}{\partial g}]^2 u^2(g) + [\frac{\partial \eta}{\partial U_m}]^2 u^2(U_m) \end{aligned} \quad (5.1.2)$$

$$\begin{aligned} u^2(\eta) = {} & [\frac{\partial \eta}{\partial D_s}]^2 u^2(D_s) + [\frac{\partial \eta}{\partial \rho_s}]^2 u^2(\rho_s) + \\ & [\frac{\partial \eta}{\partial \rho_f}]^2 u^2(\rho_f) + [\frac{\partial \eta}{\partial g}]^2 u^2(g) + [\frac{\partial \eta}{\partial U_m}]^2 u^2(U_m) \end{aligned} \quad (5.1.3)$$

That is, the maximum permitted uncertainty of the terminal velocity and viscosity measurement system becomes;

$$\begin{aligned}
u(U_{corr1}) &= (0.0095)\frac{cm}{sec} \\
u(U_{corr2}) &= (0.0126)\frac{cm}{sec} \\
u(U_{corr3}) &= (0.0098)\frac{cm}{sec} \\
u(\eta_1) &= (0.0409)centipoise \\
u(\eta_2) &= (0.0397)centipoise \\
u(\eta_3) &= (0.0376)centipoise \\
u(\eta_1) &= (0.2120)centipoise \\
u(\eta_2) &= (0.3021)centipoise \\
u(\eta_3) &= (0.2011)centipoise
\end{aligned}$$

Appendix B

A. Matlab code to plot x-coordinate position of falling spheres versus time

t1=18/60; i=1:41; t=i*t1;

x1=[2 8 15 21 25 32 36 42 49 54 58 62 70 76 80 86 91 100 104 111 120 124 130 136 141 147 152 158 163 168 173 179 188 194 200 206 210 215 222 227 230]/1.966;

x2=[3 7 13 20 28 37 44 50 55 61 66 72 78 85 89 92 97 105 109 117 122 131 131 141 145 150 155 159 164 170 176 181 188 195 196 202 208 213 218 224 229]/1.957;

x3=[3 8 15 23 28 34 40 44 49 59 63 69 74 78 83 89 98 102 105 110 115 122 128 132 138 145 151 156 160 167 171 177 182 187 191 196 206 209 211 216 221]/1.966;

plot(t,x1,'r')

hold on

plot(t,x2,'b')

hold on

plot(t,x3,'g')

B. Matlab code to plot and determine the falling velocity of a spheres

t1=18/60; i=1:41; t=i*t1;

x1=[2 8 15 21 25 32 36 42 49 54 58 62 70 76 80 86 91 100 104 111 120 124 130 136 141 147 152 158 163 168 173 179 188 194 200 206 210 215 222 227 230]/1.966;

x2=[3 7 13 20 28 37 44 50 55 61 66 72 78 85 89 92 97 105 109 117 122 131 131 141 145 150 155 159 164 170 176 181 188 195 196 202 208 213 218 224 229]/1.957;

x3=[3 8 15 23 28 34 40 44 49 59 63 69 74 78 83 89 98 102 105 110 115 122 128 132 138 145 151 156 160 167 171 177 182 187 191 196 206 209 211 216 221]/1.966;

U1=x1./t

U2=x2./t

U3=x3./t

plot(t,U1,'r')

hold on

plot(t,U2,'b')

hold on

plot(t,U3,'g')

C. Matlab code to fitted measured terminal velocity with theoretical terminal velocity versus of time for a sphere of radius(r=0.626cm) in oil

m1=2.75; m2=3.05; m3=2.89; d1=1.252; d2=1.336; d3=1.306;

r1=d1/2; r2=d2/2; r3=d3/3;

Vav=(v3+v4+v5)/3;

tou3=m1/(6*pi*visaverage*r1);

Vt3=Vav.*(1-exp(-t/tou3));

plot(t,v3,'r-')

hold on

plot(t,Vt3,'g')

D. Matlab code to determine the viscosity of Total quartz 20W50 motor oil with and with out correction factor

g=981; ruos1=2.6767; ruof=0.893; ruos2=2.4427; ruos3=2.4779; d1=1.252; d2=1.336; d3=1.306; D=3.25; Uav1=9.1182; Uav2=9.5904; Uav3=9.2439;

$Vis1 = (d1*d1*g*(ruos1-ruof)/18*Uav1)/(1-2.1044*(d1/D)+2.09*(d1/D)^3-0.95*(d1/D)^5)$

$Vis2 = (d2*d2*g*(ruos2-ruof)/18*Uav2)/(1-2.1044*(d2/D)+2.09*(d2/D)^3-0.95*(d2/D)^5)$

$Vis3 = (d3*d3*g*(ruos3-ruof)/18*Uav3)/(1-2.1044*(d3/D)+2.09*(d3/D)^3-0.95*(d3/D)^5)$

$Vis1 = (d1*d1*g*(ruos1-ruof)/18*Uav1)$

$Vis2 = (d2*d2*g*(ruos2-ruof)/18*Uav2)$

$Vis3 = (d3*d3*g*(ruos3-ruof)/18*Uav3)$

Appendix C

A. Matlab to determine the uncertainties on the measurement of corrected terminal velocity and viscosity

D=3.25; d1=1.252000; d2=1.336000; d3=1.306000; U1=9.1182000;
U2=9.590400; U3=9.2439000; U1cor=30.3188; U2cor=35.6573;
U3cor=33.0114; g=981.0000; ruos1=2.6767; ruof=0.893;ruos2=2.4427;ruos3=2.4779;
deltaU1=0.0003276;deltaU2=0.0003098; deltaU3=0.0001904;
deltaD=0.00000058; deltad1=0.00000365; deltad2=0.0000035;
deltad3=0.0000037; deltag=0.009624;
deltaruos1=0.00000003;deltaruos2=0.00000004;
deltaruos3=0.00000004;deltaruof=0.00000625;

$A1 = 1/(1 - 2.1044 * (d1/D) + 2.089 * (d1/D)^3 - .95 * (d1/D)^5)$

$B1 = (-2.1044 + 2.089 * 3 * (d1/D)^2 - 0.95 * 5 * (d1/D)^4)/D;$

$C1 = (2.1044 * (d1/D) - 2.089 * 3 * (d1/D)^3 + 0.95 * 5 * (d1/D)^5)/D;$

$A2 = 1/(1 - 2.1044 * (d2/D) + 2.089 * (d2/D)^3 - .95 * (d2/D)^5)$

$B2 = (-2.1044 + 2.089 * 3 * (d2/D)^2 - 0.95 * 5 * (d2/D)^4)/D;$

$C2 = (2.1044 * (d2/D) - 2.089 * 3 * (d2/D)^3 + 0.95 * 5 * (d2/D)^5)/D;$

$A3 = 1/(1 - 2.1044 * (d3/D) + 2.089 * (d3/D)^3 - .95 * (d3/D)^5)$

$B3 = (-2.1044 + 2.089 * 3 * (d3/D)^2 - 0.95 * 5 * (d3/D)^4)/D;$

$C3 = (2.1044 * (d3/D) - 2.089 * 3 * (d3/D)^3 + 0.95 * 5 * (d3/D)^5)/D;$

$deltaU1corr = A1^2 * deltaU1 + (-U1 * B1 * A1^2)^2 * deltad1 + (-U1 * C1 * A1^2)^2 * deltaD$

$deltaU2corr = A2^2 * deltaU2 + (-U2 * B2 * A2^2)^2 * deltad2 + (-U2 * C2 * A2^2)^2 * deltaD$

$deltaU3corr = A3^2 * deltaU3 + (-U3 * B3 * A3^2)^2 * deltad3 + (-U3 * C3 * A3^2)^2 * deltaD$

$aa1 = d1^2 * (ruos1 - ruof)/(18 * U1cor); aa2 = d1^2 * g/(18 * U1cor);$

$aa3 = d1^2 * g * (ruos1 - ruof)/(18 * (U1cor)^2);$

$aa4 = d1^2 * g/(18 * U1cor); aa5 = d1 * g * (ruos1 - ruof)/(9 * U1cor);$

$deltaVis1err = sqrt(aa1 * deltag + aa2 * deltaruos1 + aa3 * deltaU1corr + aa4 * deltaruof + aa5 * deltad1)$

$bb1 = d2^2 * (ruos2 - ruof)/(18 * U2cor); bb2 = d2^2 * g/(18 * U2cor);$

$bb3 = d2^2 * g * (ruos2 - ruof)/(18 * (U2cor)^2);$

$bb4 = d2^2 * g/(18 * U2cor);$

$bb5 = d2 * g * (ruos2 - ruof)/(9 * U2cor);$

$deltaVis2err = sqrt(bb1 * deltag + bb2 * deltaruos2 + bb3 * deltaU2corr + bb4 * deltaruof + bb5 * deltad2)$

$cc1 = d3^2 * (ruos3 - ruof)/(18 * U3cor); cc2 = d3^2 * g/(18 * U3cor);$

$cc3 = d3^2 * g * (ruos3 - ruof)/(18 * (U3cor)^2);$

$cc4 = d3^2 * g/(18 * U3cor); cc5 = d3 * g * (ruos3 - ruof)/(9 * U3cor);$

$deltaVis3err = sqrt(cc1 * deltag + cc2 * deltaruos3 + cc3 * deltaU3corr + cc4 * deltaruof + cc5 * deltad3)$

$deltaUcorraverage = sum(deltaU1corr + deltaU2corr + deltaU3corr)/3$

$deltaViserraverage = sum(deltavis1err + deltavis2err + deltavis3err)/3$

Bibliography

[1] L.D.LANDAU and E.M.LIFSHITZ, Fluid mechanics 2^{nd} edition(course of theoretical physics volume6) Butter worth-Heinemann 1987.

[2] Willian Bober and Richard A.Kenyon, Fluid mechanics John Wiley and Sons(1980).

[3] F.M.White, Fluid Mechanics, McGraw-Hill Higher Education,(2003).

[4] C.pozrikidis, Fluid dynamics: Theory, computational, and numerical simulation Kluwer Academic publisher(2001).

[5] G.K.Batcherlor, An introduaction to Fluid dynamics 2^{nd} edition(2001).

[6] R.A.Secco, M.kostic, G.E.Leblanc,et.al.. "Viscosity Mesurement" 2000CRC Press LLC.
http://www.engnetbase.com.

[7] Rober A.Granger. Fluid Mechanics,John Wiley and Sons(1985),

[8] Brookfield http://www.brook fieldengineering.com/education/. What is Viscosity.asp.

[9] Lommatzsch.T, M.Megharfi, E.Mahe and E.Devine(2001) "Conceptual study of an absolute falling-ball viscometer", Metrologia,38, 531-534.

[10] V.C.Kelessidis*, G.Mpandelis, Measurements and prediction of terminal velocity of solid spheres falling through stagnant psedoplastic liquids, powder Technol. 147(2004)117-125.

[11] N.Mordant and J.F.pintona, velocity measurement of a settling sphere, Eur.phys.J.B18, 343-352(2000).

[12] M.Jenny, J.Dusek, and G.Bouchet, instabilities and transition of a sphere falling or ascending freely in a Newtonian fluid, J.Fluid Mech., 508,(2004),pp.201-239.

[13] Julia P owen and William S Ryu, Eur.J.phys.26(2005)1085-1091.

[14] " The Measurement, Instrumentation, and Sensors Handbook" (c)1999 by CRCPress LLC.

[15] E.T.G.Bot, M.A.Hulsen, B.H.A A Vander Brule* " The motion of two spheres falling along their line of centers in a Boger fluid." J.Non-Newtonian Fluid Mech.79(1998)191-212

[16] E.Kiran, Y.L,sen " High- pressure viscosity and density of n-alkanes." Int.J.Thermophys. 13(3): 411-442(1992).

[17] G.E.Leblanc, R.A.secco" High-pressure stoke's viscometry A New in situ technique for sphere velocity determination." Rev.Sci. Instrument.66(10): 5015-5018(1995).

[18] M.J.Assael, M.papadaki, M.Dix, S.M. Richardson, W.A.Wakeham " An absolute vibrating- wire Viscometer for liquids at higher pressures." Int.J.Thermophys.12(2): 231-244(1990).